McGill UNIVERSITY

Machine Learning in Thoracic Aortic Aneurysm Risk Assessment

Lauren Kennedy

Department of Chemical Engineering
McGill University
Montreal, Quebec, Canada
Submitted August 2022

A thesis submitted to McGill University in partial fulfillment of the requirements of the degree of Master of Science in Chemical Engineering

Table of Contents

List of figures

Background and Literature Review

Article

Appendix B

List of tables

Background and Literature Review

Article

Appendix A

List of Abbreviations

AI ≡ Artificial intelligence

AscAo ≡ ascending aorta

BAV ≡ bicuspid aortic valve

CCPM ≡ cardiac cycle pressure modulus

CTA ≡ Computed tomography angiography

GPR ≡ gaussian process regression

ML ≡ machine learning

MRA ≡ Magnetic resonance angiography

MSE ≡ mean squared error

SVM ≡ support vector machine

TAA ≡ thoracic aortic aneurysm

TAV ≡ tricuspid aortic valve

TEE ≡ transesophageal echocardiography

2D ≡ 2-dimensional

Abstract

Thoracic aortic aneurysms (TAA) present a significant risk if left untreated, often leading to fatal complications. Traditional risk assessment for recommending surgical intervention in TAA is based on aneurysm diameter thresholds, between 5 to 5.5 cm. Unfortunately, this is known to be unreliable in predicting complications, with an estimated 40% of dissection and rupture cases occurring below the surgical threshold. Biomechanical metrics have been proposed which may provide a better framework for discerning risk. This study investigates the feasibility and added value of a machine learning approach to predicting biomechanical function of aortic tissue. Supervised learning models were trained using non-invasive, clinically accessible patient data as the input parameters, collected in a collaborative multi-disciplinary aortopathy clinic. The inputs include observations from medical scans, genetic panelling, family history, and physical examination metrics (i.e., BSA, BMI, blood pressure). An in-vivo stiffness metric (Cardiac Cycle Pressure Modulus - CCPM) derived from speckle track echocardiography was considered as an additional input factor. Ex-vivo measured energy loss was used as the representative output (ground truth), describing patient risk. This was measured using biaxial tensile testing on resected tissue collected from patients undergoing surgical treatment.

A preliminary set of models, using a cohort of 158 patients demonstrated the ability of a ML algorithm to incorporate multiple clinical variables to improve the prediction of the mechanical properties of TAA tissue. These provide a significant improvement when compared to the surprisingly poor correlative power of diameter-based metrics alone. Limitations of this model highlight the heterogeneous nature of the disease, which may be addressed by a larger patient cohort. Overall, the positive results of this study provide evidence to the potential success of this new approach to clinical decision-making.

Résumé

Les anévrysmes de l'aorte thoracique (AAT) présentent un risque important s'ils ne sont pas traités, pouvant mener à des complications souvent fatales. Traditionnellement, le diamètre de l'aorte est utilisé pour faire une recommandation pour intervenir chirurgicalement. Un diamètre atteignant 5-5.5 cm est le critère principalement utilisé pour effectuer cette décision. Malheureusement, ce critère n'est pas fiable concernant le risque de rupture. Il est estimé que 40% des dissections et ruptures de l'aorte surviennent en dessous du diamètre critique de 5 cm. Des mesures biomécaniques ont été développées, ce qui pourrait offrir un meilleur système d'évaluation du risque. La présente étude investigue la faisabilité et la valeur ajoutée d'une approche d'apprentissage automatique pour prédire la fonction biomécanique du tissu aortique. Des modèles d'apprentissage supervisé ont été entrainés en utilisant des données cliniques non-invasives et accessibles comme paramètres d'entrées. Ces paramètres obtenus dans le contexte d'une clinique aortique multidisciplinaire incluent des observations génétiques, de l'imagerie médicale, l'historique médicale familiale du patient et des données d'examens cliniques (e.g. IMC, pression artérielle, surface corporelle). Une mesure de rigidité aortique in-vivo (Module de Pression du Cycle Cardiaque – MPCC) dérivée d'échocardiographie STE (Speckle-tracking echocardiography) a été utilisée comme paramètre d'entrée additionnel. Une mesure de perte d'énergie a été utilisée comme paramètre de sortie représentative (vérité confirmée), décrivant le risque pour le patient. Ces données ont été mesurées avec une machine d'essai de traction biaxiale sur des échantillons d'aorte de patients ayant reçu une chirurgie de réparation d'aorte.

Plusieurs modèles utilisant une cohorte de 158 patients ont démontré la capacité d'un algorithme d'apprentissage automatique d'incorporer plusieurs variables cliniques pour améliorer la prédiction des propriétés mécaniques de tissus d'AAT. Ces modèles offrent une amélioration

significative comparé à la corrélation assez pauvre du diamètre seul. Les limitations de ce modèle démontrent la nature hétérogène de la maladie, ce qui pourrait être adressé par une plus grande cohorte. Globalement, les résultats positifs de cette étude témoignent du succès potentiel de cette nouvelle approche aux prises de décisions cliniques.

Acknowledgement

I would like to sincerely thank my supervisors Prof. Richard Leask and Dr. Kevin Lachapelle, for their support and guidance throughout these past two years. I would also like to thank the members of the Leask Lab, with a special thanks to Matt Halloran and Melissa Dick, for words of encouragement when they were most needed.

I want to especially thank Kevin Bates, who is a rock star. Thank you for helping to train me and then continually provided collaborative ideas, support, and friendship throughout this project.

To all the clinicians, cardiologists, and fellows, whom I have had the pleasure of learning something from throughout this experience, thank you.

To my parents, Elaine and Dallas, I would genuinely be nowhere if it weren't for your endless support and confidence in me.

To my roommates in apartment 94, Sophie Masson, Mekayla Forrest, Lucy Penney, Jennifer Duffy, and Elizabeth Flynn, thank you for creating a family for me in Montreal, throughout the waves of Covid-19 lockdowns and phases of this degree.

Finally, thank you to my loving partner, Evan, who was there every step of the way.

Contribution of Authors

Article 1 – Thoracic Aortic Aneurysm Risk Assessment: A Machine Learning Approach

Contributions:

Lauren Kennedy – performed the experiments, collected, analyzed, and interpreted the data, wrote, and edited the manuscript.

Kevin Bates – assisted with experiments and the collection of data

Judith Therrien – provided clinical feedback, supervised clinical data collection, reviewed the manuscript

Yoni Gros – assisted with the collection of data and provided clinical feedback

Masaki Kodaira – assisted with the collection of data and provided clinical feedback

Josephine Pressacco – assisted with the collection of data and provided clinical feedback

Anthony Rosati – assisted with the collection of data

Tara-Lyn Lewis – facilitated clinic for data collection

Kevin Lachapelle – surgeon, co-directed the research, supervised clinical data collection, provided funding and contributed to editing and revising the manuscript

Richard L. Leask – co-directed the research, provided funding and contributed to editing and revising the manuscript

Chapter 1: Introduction

The aorta is the largest artery in the human body, acting as the distribution conduit for all other major arteries. It delivers oxygenated blood to the body by the pressure created by the hearts left ventricle. The aortic valve, a tricuspid valve connected to the left ventricle, prevents regurgitant blood flow from the aorta back to the heart (1). Complications of thoracic aorta and/or aortic valve jeopardize blood supply to the entire body.

The function of the thoracic aorta can be characterized in terms of its elastic properties. In addition to acting as a vessel, the thoracic aorta acts as a buffer, by pulsating in sequence with the beating of a heart. The aorta expands during systole and contracts during diastole, to facilitate continuous blood flow (1, 2) between heart beats, the Windkessel effect.

The aortic wall is made up of three defined tissue layers, with the middle and thickest layer, the media, facilitating the aorta's elastic function. The medial layer of the tissue naturally undergoes remodelling overtime with aging (3), causing the dilation and increased stiffness of the aortic wall (4, 5). An aortic aneurysm is defined as a dilation that exceeds the natural adult diameter by 50% due to abnormalities in tissue remodelling (6). Aortic aneurysms commonly lead to fatal complications, specifically dissection and ruptures. A dissection is the splitting of the layers of the arterial wall, allowing the build-up of blood within the vessel lining, and rupture is a bursting of the vessel (7).

Aortic aneurysms and dissections were found to be the cause of 9,900 deaths a year in the US in 2019, by the Center of Disease Control and Prevention (8). Aneurysms located in the thoracic

aorta, the upper segment of the aorta located in the chest, are less common than those in the abdomen, having an incidence of approximately 7.6 per 100 000 patient year, however, reported cases have been found to be increasing over recent years (9). Thoracic aortic aneurysms (TAA) are clinically important because of the high risk of catastrophic complications (10). Aortic dissections in the ascending aorta (AscAo) have a mortality rate of 57% without treatment, and a 17-25% mortality rate with emergency surgery (11). Elective surgical intervention has a much lower risk of mortality and can be lifesaving to at risk individuals. Mortality rates for prophylactic repair of ascending aortic and aortic root aneurysms are approximately 1% in experiences centres(12). However, elective repair of asymptomatic TAA is not recommended until the risk of rupture or dissection exceeds the risks associated with the repair.

Current guidelines for determining at risk patients are largely based on aortic diameter thresholds, between 5 and 5.5 cm, varying based on different pathologies of the disease (12). The use of maximum aortic diameter has been brought into question as being a poor predictor of at-risk aortas, with approximately 40% of all ascending aortic dissections occurring below 5 cm, and 60% below 5.5 cm (13). One study found that degenerative aneurysms have a zero percent risk of rupturing in 5 years only below a diameter of 4 cm (14). With 4 cm being the lower threshold, yet 5.5cm being the cut off for surgery, there is a significant gap in patients that have some degree of risk who are not considered severe enough to undergo elective treatment. Furthermore, another study found the median diameter of rupture or dissection in patients studied with TAA to be 6.0 cm (15), indicating that there are patients above the surgical threshold who are not at significant risk. All these studies highlight the flaws of using such an oversimplified method of quantifying patient risk.

Complications such as dissection and rupture are essentially methods of mechanical failure in the vessel. By this logical, metrics describing the biomechanical state of the tissue may be a better framework for assessing patient risk (16). Many studies have been performed to link the mechanical properties of aneurysmal tissue to the pathology of the patient's disease (17–19). In particular, a previous study has linked an ex-vivo measured biomechanical tissue metric, energy loss, to the histopathological state of the medial layer in the tissue (7). The energy loss has been shown to effectively differentiate between patients with elevated medial degeneration to an intact tissue structure at similar diameter levels. Functionally, the energy loss describes the elastic energy lost in the tissue each cardiac cycle.

A reliable method of predicting energy loss in vivo could be the next step in providing clinicians with a more robust metric of patient risk, to assist in the decision-making process. The use of ultrasound imaging has been utilized previously to estimate stiffness of the aortic tissue, however, currently an accurate in vivo prediction of energy loss has not been attempted (20). The energy loss has shown to be a more robust ex vivo metric than ex vivo stiffness.

In recent years, there has been an increasing interest in machine learning (ML), a subset of artificial intelligence (AI), for its promise for improving patient risk assessment (21). This technique has been investigated in numerous applications of cardiovascular disease, showing improvement over traditional methods of risk prediction in many cases (22–24), one example being the detection of arterial fibrillation in heart-rate monitoring data from wearable sensors in smart watches (25). The use of a biomechanical metric as the predictive output of a model would

allow for the continued intervention of patients who are traditionally considered at risk, while producing a measure of aortic function which can be predicted in vivo.

Chapter 2: Objectives and Hypothesis

This thesis is driven by the general hypothesis that the pathology of aortic tissue, as described by its biomechanical state, is a better predictor of complications than the size of the aorta. With this being the case, an in-vivo clinically accessible method of predicting the biomechanical state of a given patient's tissue is desired. Promoting the specific hypothesis tested in this thesis, that the biomechanical state if the tissue can be affectively accessed using ML techniques.

The primary objective of this thesis is to investigate the feasibility and added value of using a ML approach to predict the function of TAA tissue in vivo, from patients' clinical information. The ex-vivo measured energy loss will be used as the representative output (ground truth), measured by biaxial tensile testing of surgically resected tissue. Input data for this study will use information from a clinical database collected by a multidisciplinary aortopathy clinic; including physical examination metrics, observations from medical scans, comorbidities, family history and genetic test results. Additionally, a stiffness modulus found by a speckle tracking echocardiographic analysis, called the cardiac cycle pressure modulus (CCPM), will be included as a potential input.

The following are the main questions of interest in this study:

1. Can ML be used to accurately predict energy loss of TAA patients from only clinical data? How does this prediction compare to other currently used clinical metrics?
2. What are the key clinical factors that are significant to the model?
3. Does the inclusion of CCPM improve the prediction of the ML model?
4. What are the main challenges and limitations found by this approach? How feasible would it be for this method to be adopted by the field as a clinical decision support system?

Chapter 3: Background and literature review

3.1 Risk Management in Thoracic Aortic Aneurysms

3.1.1 Current clinical guidelines and metrics

Thoracic aortic aneurysms (TAAs) are brought about by many mechanisms but are most often classified as being either senile degenerative or triggered by a genetic predisposition (6, 26). Genetic cases are typically seen in younger patients, and most commonly present as either Marfan's syndrome, Loeys-Dietz syndrome, non-syndromic familial aortic disease, and aortic valve malformations. The suspected cause of the aneurysm has a significant impact on the assessment of patient risk, as there are different trends in the growth rate, and stability of condition among these different patient groups (10, 12).

Aortic aneurysms in older patients are typically degenerative, and associated with other cardiovascular issues like atherosclerosis, hypertension, smoking, and old age (6, 10). Despite the strong association, not much is known about the specific pathogenesis of TAAs (24). In contrast with this, genetically triggered aneurysm syndromes are typically seen in younger patients (27). Marfan syndrome and Loeys-Dietz are connective tissue disorders which have been well characterized for their identifying genetic variants and mechanistic roles (27–29).

Valve malformations, such as bicuspid aortic valve syndrome (BAV), have been seen to have a significant impact on the histopathology of the AscAo with aneurysms commonly presenting early in life, in up to 26% of patients having this deformity (30, 31). There is evidence to support that the disease progression in bicuspid aneurysms can be influenced by both genetic and hemodynamic factors (32, 33).

Approximately 20% of patients who develop TAA have a family history of aortic disease, without meeting the criteria for a genetic syndrome (10). These patients typically present at a younger age than natural forming aneurysms, but at an older age than those having other connective tissue disorders (27). They also typically have faster growth than those with degenerative aneurysms (10). Some causative genetic variants have recently been defined for this subset of patients; however, mechanistic details are only partially known (27) and for a large portion of these patients a causative genetic variant has not yet been identified (34).

Current clinical guidelines for recommending surgical intervention use the greatest diameter of the aorta as the most important decisional criteria, using a threshold value of 5.5 cm (12). For patients being considered at an increased risk, such as those who are determined to have a genetic predisposition, a lower size threshold is considered, and patient risk is assessed on a more individual basis. Patients with known genetic variants have a range of reduced thresholds proposed, based on the affected gene (35). In addition to this, patients presenting with additional risk indicating factors, such as heart failure symptoms or rapid growth in aortic diameter (> 0.5 cm/yr), are considered as a special circumstance(12).

Several other metrics have been recommended in the literature over time, including aortic size index (ASI) (aortic size/BSA) (36), aortic height index (AHI) (aortic size/height) (37), and aortic surface area/height (38–40). Proposed thresholds are summarized in table 1.

Table 3.1: Current recommended thresholds for assessing risk in asymptomatic TAA

Risk Metric		**Threshold**	**Comments**	**Ref.**
Ascending aortic size (mm)	Sporadic	5.5		(12)
	Genetic	4.0-5.5	Depending on gene	(12)
	BAV	4.5	Combined with severe AS or AR	(41)
		5	Combined with additional risk factor (ie. Family history)	
		5.5	No additional risk factors	
Ascending aortic size/BSA (cm/m^2)		2.75	Moderate risk	(36)
		4.25	High risk	
Ascending aortic size/height (AHI) (cm/m)		3.70	Moderate risk	(37)
		4.35	High risk	
Aortic surface area/height (cm^2/m)		10		(38–40)
Growth rate (cm/yr)		0.5		(12)

AR = aortic regurgitation, AS = aortic stenosis, BAV = bicuspid aortic valve, BSA = body surface area, TAA = thoracic aortic aneurysm

3.1.2 Physiology

The aorta is made up of three main layers, the inner-most layer being the intima, which is lined by a single layer of endothelial cells, the media, and the adventitia which is mainly made up of collagen. The medial layer of the healthy tissue is made up of alternating concentric layers of cross-linked elastin fibers (42). Within these layers are bundles of collagen, smooth muscle cells, and mucopolysaccharides (see figure 3.1). These layered elastin fibers facilitate the elastic function of the tissue (43).

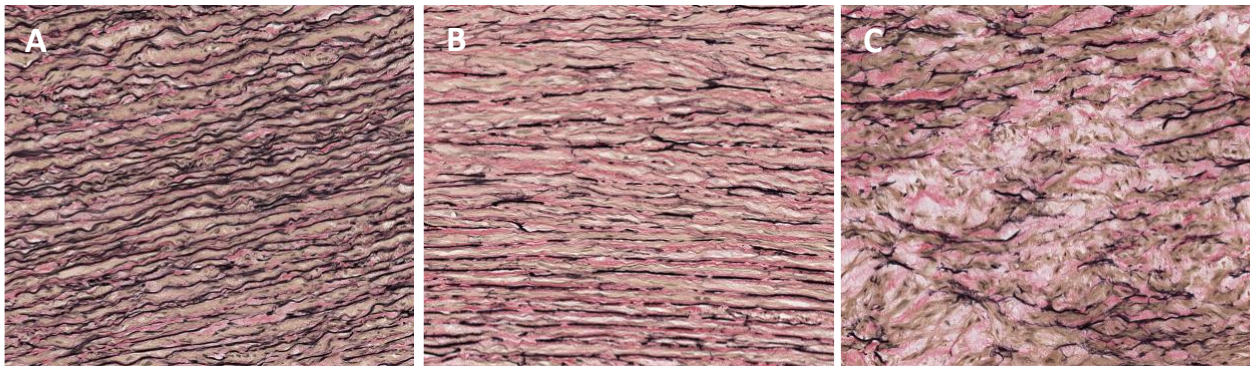

Figure 3.1: Histopathology of the ascending aorta using Verhoff straining in (A) A 59-year-old with a non-dilated ascending aorta, (B) a 73-year-old with a 5.9 cm ascending aortic aneurysm, and (C) a 26-year-old diagnosed with Marfan syndrome, having a 5.8 cm ascending aortic aneurysm. **Black** indicates elastin and cell nuclei; **red** indicates collagen; and **yellow** indicates cytoplasmic elements.

As the aorta ages, it naturally dilates overtime, without losing thickness on the wall, meaning that the area of the aortic wall is increasing with time (42, 44). As a result, the density of the elastin fibers and smooth muscle cells is decreased, while it is thought that the total amount likely stays the same (45, 46). This increased area is thought to be made up by increased collagen deposition in the tissue (42). Collagen fibers are much stiffer than elastin fibers, and therefore, as a result, the stiffness of the tissue is gradually increased with aging (47). There is also evidence to the fragmentation in the elastin fibers and increased medial fibrosis in elderly individuals (45).

Degeneration of the medial layer in the diseased aorta is typically characterized by a loss of smooth muscle cells and the fragmentation of the elastic fibers (26). Similarly, to aging, the aorta typically maintains its thickness while dilating, resulting in the increased deposition of collagen

fibers (18, 42). The degree of medial degeneration and thickness of the tissue wall can vary greatly among different regions in the vessel (18, 48, 49).

In cases of connective tissue disorders, aneurysms develop due to genetic mutations that disrupt the pathway to produce the healthy tissue structure. For example, in Marfan's disorder, the gene encoding a protein responsible for elastin fiber assembly is mutated (50). As a result, Marfan's can be characterized by a severe fragmentation and loss in the layered elastin structure (51).

These different pathologies within the disease each correspond to different mechanisms by which this dilation and stiffening of the tissue occurs. Therefore, these different pathologies carry different interpretations of their respective risk (26).

3.1.3 TAA Characterization with Biomechanical function

Aortic diameters are used as a surrogate for a biomechanical metric, based on Laplace's law, which states that the wall stress within a vessel (σ) is directly proportional to the aortic radius (r) assuming the pressure exerted on the vessel wall (P) and the wall thickness (τ) are constant (16).

$$\sigma = \frac{P\,r}{\tau} \qquad \text{Where } r \gg \tau$$

Therefore, the larger the diameter of an aorta, the greater the stress on the aortic wall. This equation applies to a thin-walled sphere or cylinder, having a uniform shape and dispersion of pressure. Unfortunately, this is an oversimplified approach to be used in TAA, where the vessel has nonuniformities in the shape, wall thickness, and hemodynamic pressure (18). This is also intended for a material having a linear stress/strain relationship, where the material structure is homogeneous. While the aortic wall is a heterogeneous structure, having a viscoelastic stress-

strain relationship, which also undergoes remodeling concurrently with vessel growth (52). Finally, this approach treats all individuals the same, despite there being natural differences in the healthy aortic size among individuals of different sex, ethnicity, lifestyle and body size (53).

The function of the aorta can be characterized instead in terms of its elastic properties, as described by the Windkessel function (1) (Figure 3.2). During systole, as blood enters the aorta, its walls elastically deform to expand in response to the increased radial pressure, storing a larger volume of blood as a result. During diastole, the aortic wall slowly recoils back to its original state, transferring elastic energy into the stored volume of blood now being pushed into circulation (1, 2). As a result, blood flow remains nearly constant despite the non-continuous action of the heart.

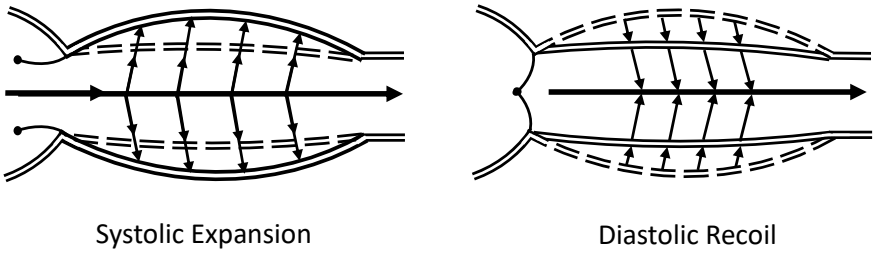

Figure 3.2: Stages of aortic wall deformation in accordance with the Windkessel function. Diagram adapted from Belz, GG (1995)(1)

To better characterize this biomechanical nature of the thoracic aorta, studies have used several methods of ex vivo, in vivo, and computational analysis.

3.1.3.1 Ex Vivo studies

Ex-vivo mechanical testing studies mainly consist of uniaxial and biaxial tensile testing. This is a method where a material is deformed, either in 1 axis or 2 axes, and the force required to stretch the tissue a given distance is recorded. This approach provides stress-strain data on the tissue and allows for the determination of metrics including elastic stiffness modulus at different degrees of deformation (54), ultimate tensile strength (55, 56), anisotropy (57, 58), and energy loss (16, 59).

Aortic tissue is hyper-elastic, meaning there is a nonlinear relation between stress and strain, forming a curve, as shown in figure 3.3. In addition to this, the tissue is viscoelastic in nature, meaning that the stress strain curves follow different paths during loading and unloading, forming a hysteresis loop (16). The stiffness of the tissue can be assessed at any point of the cycle, by the tangential slope of the stress-strain curve. The ultimate tensile strength is the maximum strength that is reach by the tissue before breaking.

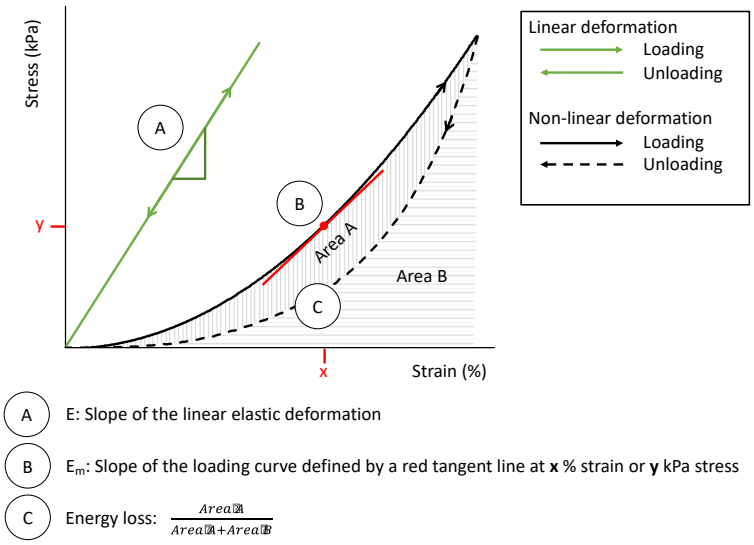

Figure 3.3: Typical shape of stress-strain curve for linear elastic (Green line) and viscoelastic response of biological tissue (black line). A) Elastic modulus of a linear elastic material, B) Incremental stiffness modulus of a non-linear material and C) Energy loss. Figure and caption adapted from Emmott, et al.(16)

Bi-axial tensile testing is particularly useful for its relative comparability to the physiological environment of the aorta (60), allowing for mechanical inferences to be made about the behavior of the tissue during the cardiac cycle in vivo. This testing method has allowed researcher to distinguish mechanical trends between the longitudinal and circumferential axis (57, 58), aortic regions (17, 18), and disease pathologies (19). Aneurysmal aortas are repeatedly found among these studies to have a higher stiffness and a lower ultimate tensile strength when compared to age matches controls in both axis (55, 56, 61).

These measurements are useful for making general comparisons between studies; however, stiffness values cannot be readily compared with one another unless they are taken at the same point on the curve, because of the non-linear nature of the stress-strain relation (16).

For this reason, another metric known as the energy loss, or energy storage, of the tissue has been investigated. It corresponds to the energy that is not returned to the blood during the cardiac cycle, in accordance with the Windkessel function (1). This value can be measured ex vivo by the area of the hysteresis loop formed between the loading and unloading curves of the stress-strain profile (7). This method has the benefit of being self-normalizing, as it is an integral metric over the full cardiac cycle, unlike tissue stiffness. Like stiffness, this metric has been shown to be elevated in diseased vs. control patients, however, more importantly, this measure has been found through histological analysis to correlate to the ratio of collagen to elastin to the medial layer of the tissue (7).

These biomechanical indexes (such as stiffness, stress/strain relation, and energy loss) provide insight into the pathology of the aorta. It is important to note however, that there is no clinical or epidemiologic demonstration of its ability to directly predict dissection or rupture. With this said, ex vivo analysis remains an important step in understanding the mechanical behaviors of aortic tissue. However, its clinical applications are limited in that it can only be performed postoperatively.

3.1.3.2 In Vivo predictions of Biomechanics

A range of studies have proposed techniques for the interpretation of mechanical properties in vivo, mainly through echocardiography, computed tomography angiography (CTA), and magnetic resonance angiography (MRA), with the additional incorporation of computational fluid mechanics.

Many studies have employed the use of ultrasound imaging, particularly echocardiography, due to its ability to easily track the aortic walls while in motion(62). Transthoracic ultrasound can be gathered non-invasively, however, to avoid interference by the sternum or ribs, transesophageal ultrasound is also employed. Stiffness within the aorta can be estimated through a range of metrics, including pulse wave velocity, distensibility, and stiffness. Pulse wave velocity, being the ratio between the transit distance and transit time of a pressure wave between two sites in the arterial system has been measured non-invasively using Doppler echocardiography(63, 64).

Estimates for aortic distensibility and stiffness have been demonstrated using Motion mode and 2-dimensional (2D) ultrasound techniques, wherein the change in aortic diameter is noted in tandem with an aortic pressure line to create a rough stress-strain relation(65, 66). In 2D ultrasound a speckle tracking technique can be used, which uses acoustic markers to track the wall deformations over the whole cardiac cycle, to provide a more accurate measure of strain. A study performed by Emmott et al., using speckle tracking transesophageal echocardiogram (TEE) to estimate aortic stiffness demonstrated a correlation with ex-vivo measured energy loss and histopathologic elastin-to-collagen content(20).

Echo visualization is often obstructed, and difficult to accomplish, therefore, methods of CTA and MRA have been investigated for their higher spatial resolution(62). CTA and MRA are largely used for patient specific models of the aorta, utilized with ECG gating to provide a better understanding of local wall deformations(67–69). Through this method it is possible to produce a full strain field over the cardiac cycle, allowing for patient specific local differences in distensibility and stress concentrations on the aortic wall to be determined(67, 69).

Many recent studies have utilized more sophisticated techniques such as 4D flow MRA (70–72). This imaging method is capable of quantify vessel deformation and blood flow velocities over the cardiac cycle. This has resulted in studies which have provided evidence to the importance of hemodynamic load and patterns on aneurysm development(73–76). Computational fluid mechanics have been employed as well, specifically, using a method called fluid structure interaction, which simultaneously simulates blood flow and wall deformations. This can be used in tandem with imaging techniques to produce patient specific simulations that determine values for hemodynamic metrics, including velocity, pressure, and wall sheer stress (77–80).

With recent improvements, clinical imaging techniques are becoming increasingly useful for assessment tissue dysfunction, however, these interpretations have limitations. The main limitation being a simplified estimation of the stresses acting on the tissue over the cardiac cycle(16). In vivo predictions of stiffness are useful; however, this metric lacks the robustness required to make a confident assessment of patient risk. More sophisticated methods of found by CTA an MRA using patient specific models have many useful applications for assessing unique

cases, however, they are also very time costly, which could be a drawback in their integration into larger scope clinical decision making.

3.2 Machine Learning in Cardiovascular Disease

3.2.1 Machine Learning Overview

ML is a subset of artificial intelligence (AI) which is increasingly gaining attention for its range of applications in the medical field. This is a method of computational modelling where large-scale pattern recognition is used to determine trends within a data set(81). This technique takes a non-parametric approach to predictive modelling, allowing it to be continually learning with the addition of new information (figure 3.4)(82, 83).

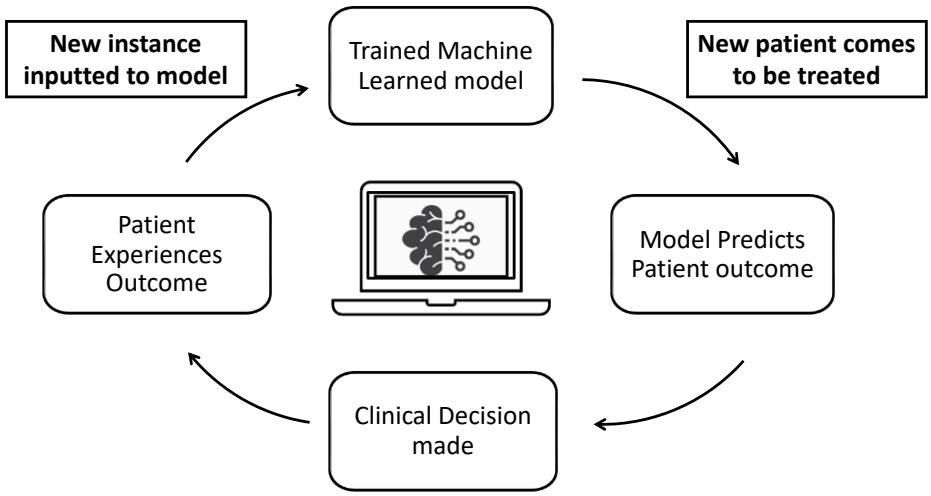

Figure 3.4: Learning cycle of a predictive machine learning model

The term ML describes the workflow by which a model is created and the continual learning nature of the final product. The actual computer algorithm used to create the model can vary greatly, ranging in complexity from simple linear regression to complex algorithms such as

neural networks. There are two main types of ML, which include unsupervised and supervised learning (figure 3.5)(81). Unsupervised learning is used to extract patterns from complex data sets, to help give a better understanding of what relationships exist within the data. This can be used on its own, as a method of identifying patterns in a patient cohort, or it can be used as a preliminary step to supervised learning. Supervised learning is used to relate the collected data to a specific outcome. The product of supervised learning is a computer model, which can then be used to predict the specific outcome for a new instance, or patient. Supervised learning models have two main types, classification, and regression, where the outcome of the model is either a discrete category or a continuous value, respectively.

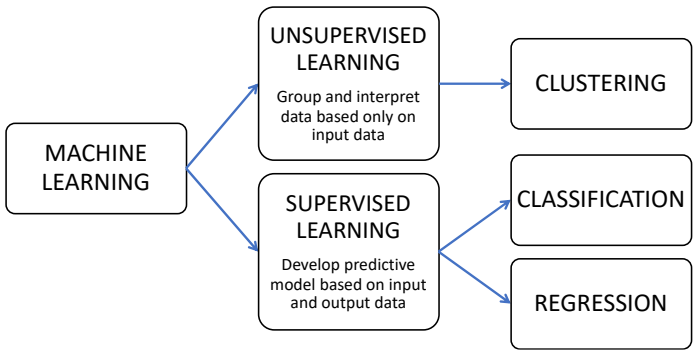

Figure 3.5: Breakdown of machine learning techniques, adapted from Matlab™ (2016)(81)

The typical workflow to produce a supervised learning model includes the collection and pretreatment of data, the employment of dimensionality reduction techniques, model training, and then model validation. Typically, in the production of a model, very large data sets having many variables are initially collected. Techniques can then be used to determine the most significant variables for predicting the desired output to be used in the model. These techniques are referred to as dimensionality reduction techniques, as they reduce the overall complexity

within the problem(84). There are dozens of possible techniques available, which can be statistical or computational in nature(85).

Model performance is assessed through model validation and model testing (85). Validation is performed during training, as a method of quantifying change in performance with changes in variable selection and hyperparameters. This can either be done by having a left-out validation set of data or by cross validation. Cross validation is an averaging method, which estimated model performance while still training a model with all available data(21). Model testing is performed after training is complete, using a dataset that has been completely left out, to assess the generalizability of the model (85).

3.2.2 Uses of Machine Learning in Cardiovascular Disease

The projected market for AI technology in health care is expected to grow from $2.1 billion to $36.1 billion by 2025 (86). There is a rapidly increasing interest in the implementation of big data and ML for care in medicine. As cardiac surgery is already a high-tech field of medicine, its interest is particularly high (87). Having rigorous screening, numerous stages in patient care, and a heavy focus on computerized risk scoring, there are many possible applications.

Unsupervised learning in cardiovascular disease has been mainly used for the purposes of phenotypic classification of patient groups, from their clinical assessment, laboratory testing, socioeconomic factors, and medical imaging-based observations (88–91) . There is a large range of supervised ML applications in cardiovascular medicine including automated image interpretation, natural language processing, data extraction from electronic health records, and

predictive analytics (85). For the purposes of this study, predictive analytic based models for cardiac disease and surgery will be the focus of discussion.

3.2.2.1 Unsupervised Learning in Cardiovascular Disease

Unsupervised learning occurs when a group of input data is considered, with no assigned outcome, for the purpose of determining trends and relationships within a data set. This is used when there is no prior knowledge of the groups within which these patients belong. The most common unsupervised learning method used is data clustering. This is a method of dividing a dataset into groups, based on dissimilarities among the datapoints. This can provide insight into the phenotypes of a disease, without the influence of the investigator's preconceived ideas (92).

This method allows a way to explore the heterogeneity within a disease category and can help determine trends in patient outcomes among the found distinct groupings. For example, one study conducted by Kwak, et al. performed a cluster analysis on patients having severe aortic stenosis based on clinically accessible data. Comparing the resultant outcomes of the patients within the separate clusters showed a significant difference in the instance and cause of mortality among the groups (88). Models have also been created looking more heavily based on medical scanning observations, with one study using CTA reconstructions to determine distinct phenotypes in bicuspid aortopathies. Subgroups were found based on the primary location of aneurysmal dilation in the aorta (90).

3.2.2.2 Prediction based Supervised Learning models in Cardiac Disease

There are increasing numbers of studies currently underway for the use of supervised ML for its use in risk prediction in relation to various components of cardiac surgery and disease.

Many supervised learning models for cardiac surgery use a classification approach to determine in a yes or no fashion if a patient is predicted to undergo a given outcome. Many for the purposes of predicting patients' risk of surgical mortality (93–95). For example, Allyn et al used clinical data to predict patients intrahospital mortality after elective cardiac procedures, to a better accuracy than EuroSCORE II (94). Kilic et al (2020) investigated the use of ML to predict the mortality risk during CABG surgery, on a cohort of 11,190 patients, using common clinic markers, showing improvements over the currently used STS PROM model (95). Studies have also looked at applications relating to in-hospital logistics such as length of in-hospital stay, and 30-day hospital readmission(96, 97).

Risk prediction for patients for the intention of guiding clinical decision making has also been attempted (22, 98). In one study, a model for screening and assessing cardiovascular risk in young asymptomatic individuals based on clinical and laboratory inputs was investigated, using the presence of subclinical atherosclerosis as the output representing risk (23). Another study used biochemical observations from patients' blood tests to predict risk level of patients for developing cardiovascular disease, using a cardiac risk level decided by health care professionals as the representative output (24). Huo et al proposed a model based on patient demographic information and blood test results for suspecting aortic dissection, when a patient initially arrives

at emergency care, to ensure higher risk patients have faster diagnosis by medical imaging to provide more timely care(99).

The temporal nature of data can also be considered when modelling, a factor that is known to be an important consideration in cardiac disease (27, 100). A study by Choi, et al. looked at the changes in metrics from medical records with time as a consideration for predicting patient heart failure (101).

3.2.3 Limitations of Machine Learning

Despite the interest in ML applications in health care, there are many challenges that need to be addressed. Implementing ML approaches into medical practice, especially with respect to risk prediction models, need to be heavily monitored, especially in cases where they relate to life threatening complications and conditions. For these cases modelling should serve to supplement interpretation of data rather than replace the human aspect of care, acting as decision support instead of decision-making systems. False predictions by the model could potentially lead to catastrophic outcomes for patients and therefore every case needs careful monitoring. For this reasons ML can more likely be implemented where prediction is already largely dependent on logistic regression models, as a way of improving these further(85).

An additional challenge is that many ML models are not easily interpretable. Physicians need to know the significance of risk factors within the prediction model, however, in many algorithms' interpretation is not simple like in a logistic regression. This difficulty in understanding where prediction comes from makes it difficult for physicians to trust them (85).

Modelling is limited by the need for large amounts of consistent data. In Cardiology in particular, there are known to be large variations in treatment throughout the field, with differences in aspects such as testing and intervention rates between centers, access to care among different socioeconomic demographics, and differences in methods of medical scanning and measuring geometries (102–105). These inconsistencies limit the potential accuracy of computer modelling.

Chapter 4: Thoracic Aortic Aneurysm Risk Assessment: A Machine Learning Approach

Preface

This chapter was prepared with the intention of being submitted as a manuscript to the Journal of the American College of Cardiology. As discussed in Chapter 3, the clinical treatment of TAA has been historically guided by simple numerical indexes which are meant to act as a correlative measure to patient risk. Other in-vivo interpretation of patient risk, based on the biomechanical function of the tissue, have been attempting, using approaches mainly focused on medical imaging. Although useful, many of these techniques are time costly and cannot be easily performed in a clinical environment, requiring patient specific reconstructions, estimations of aortic wall thickness, and access to specific imaging processing software.

This study proposes the use of regression-based machine learning (ML) to create a new correlative measure of patient risk, using clinically accessible patient information as the primary input values. The ex-vivo measured biomechanical metric, energy loss is proposed as the predicted output of the model, representing the relative risk of the patient. The model was trained using a cohort of 158 patients who received elective aortic resection surgery, at the McGill University Health Center. The correlative performance found by a variety of ML model types were compared to that found by simpler linear regressions based on currently considered size metrics. Additionally, the combination of this method with an echocardiogram based in-vivo analysis proposed by Emmott et al (2018) was investigated, demonstrating the different benefits seen between these two procedures.

This study demonstrates a workflow for producing a correlative measured of aortic function that could be easily applied into the clinical environment as a simple desktop application. Patient information can be inputted at the time of clinical assessment, and the predicted energy loss would be immediately returned. Providing a simple screening tool which can be easily applied on a large scale, identifying those individuals who are expected to be at an abnormally high risk, for closer consideration.

Article

Thoracic Aortic Aneurysm Risk Assessment: A Machine Learning Approach

Machine Learning in Thoracic Aortic Aneurysm Management

Lauren Kennedy, BEng[a,c], Kevin Bates, MSc[a,c], Judith Therrien, MD, FRCPC[b], Yoni Gros, MD[b] , Masaki Kodaira, MD[b], Josephine Pressacco, MD, PhD[d], Anthony Rosati, BEng[a,c], Tara-Lyn Lewis, LPN[c], Kevin Lachapelle, MD, FRCSC[c], Richard L. Leask, PhD[a]

Word Count: 4980

[a]Department of Chemical Engineering, McGill University, Montreal, QC, Canada

[b]Division of Cardiology, McGill University Health Centre, Montreal, QC, Canada

[c]Division of Cardiac Surgery, McGill University Health Centre, Montreal, QC, Canada

[d]Division of Radiology, McGill University Health Centre, Montreal, QC, Canada

Funding: MUHC Foundation ARAP Study, NSERC Discovery Grant 2018-06161

Disclosures: None

Address for correspondence: 3610 University St., Montreal, QC, Canada, H4B 0CA

Acknowledgements: MUHC Aortic Clinic Patients and Staff (Dr. Benoit de Varennes, Carole Albert, Dr. Kent MacKenzie, Dr. Oren Steinmetz, Alexander Emmott, Dr. Ali Alakhtar). Dr. Francois Dagenais from the Institut Universitaire de Cardiologie et de Pneumologie de Quebec.

Abstract

Background: Traditional methods of risk assessment for thoracic aortic aneurysm (TAA) based on aneurysm size alone have been called into question as being unreliable in predicting complications. Biomechanical function of aortic tissue may be a better predictor of risk.
Objectives: This study investigates the feasibility and added value of using a machine learning (ML) model as an in-vivo correlative measure of ex-vivo TAA biomechanical function.
Methods: Biaxial tensile testing was performed on resected TAA tissue, collected from patients undergoing prophylactic surgery. The energy loss of the tissue was calculated and used as the representative output. Input parameters from pre-operative patient assessments included observations from medical scans, genetic panelling, and physical examination metrics.
Results: A total of 158 patients were included in the analysis (mean age 62, ranging 22-89, 78% male), including 11 healthy controls. Mean ascending aortic diameter was 47±10 mm, with 46% having bicuspid aortic valves. Four ML algorithms were trained in Matlab^{TM}. The best performing model was found to give a greater correlative measure to energy loss (R^2:0.63) than the surprisingly poor performance of aortic diameter (R^2:0.26) and indexed aortic size (R^2:0.32). An echocardiogram derived stiffness metric was investigated on a sub-cohort of 67 patients, as an additional input, improving the correlative performance, from R^2:0.46 to R^2:0.62.
Conclusions: A preliminary set of models demonstrated the ability of a ML algorithm to improve prediction of the mechanical function of TAA tissue. This model can use patient data obtained in the clinic to provide additional information for surgical decision making.

Condensed Abstract:

Traditional risk assessment for a thoracic aortic aneurysm is based on aneurysm size, but unfortunately this is known to be unreliable in predicting complications. Biomechanical metrics have been proposed which may provide a better framework for discerning risk. This study demonstrates the feasibility of a machine learning approach to predicting biomechanical function of aortic tissue through clinically accessible, non-invasive patient data. A cohort of 158 patients justifies the added value of using an integrated model over diameter-based metrics alone in predicted ex-vivo measured energy loss. The results provide evidence to the potential success of this new approach to clinical decision-making.

Key Words: Aneurysm, Biomechanics, Machine Learning, Ascending Aorta

Abbreviations: AscAo, BAV, CCPM, GPR, ML, MSE, SVM, TAA, TAV, TEE

Abbreviations:

AscAo ≡ ascending aorta

BAV ≡ bicuspid aortic valve

CCPM ≡ cardiac cycle pressure modulus

GPR ≡ gaussian process regression

ML ≡ machine learning

MSE ≡ mean squared error

SVM ≡ support vector machine

TAA ≡ thoracic aortic aneurysm

TAV ≡ tricuspid aortic valve

TEE ≡ transesophageal echocardiography

Introduction

Thoracic aortic aneurysms (TAA) are associated with fatal complications, with a complex etiology that include both degenerative and genetic factors (1). The only method of treatment for those at risk of complication is prophylactic surgical intervention. Current surgical guidelines are based on aortic diameter with a threshold of 5.0-5.5 cm as the main decisional criterion (2, 3). These thresholds have been found to be a poor predictor of risk, with approximately 40% of all ascending aortic dissections occurring below this diameter (4). Aortic diameter as a guideline is confounded by its natural variation with sex, age, and body size. Unfortunately, much is still unknown about what discerns the level of risk in these patients, highlighting the need for new robust metrics to better guide clinical decision making.

Biomechanical metrics have been proposed as a more precise prediction model for risk of complication. Ex-vivo analysis of TAA tissue has shown biomechanical properties to correlate with the extent of medial degeneration within TAA tissue, effectively differentiating between patients with better or worse histological tissue structure at similar diameter levels (5). Medical imaging paired with simultaneous blood pressure monitoring can be used to estimate tissue biomechanical properties (6–8). However, biomechanical properties are also known to vary with patient sex, age, and genetic variants (9–11). Over and above size, it would therefore be important to be able to predict the biomechanical function prior to aortic resection. This would help identify the truly high-risk patients on either side of traditional sized-based surgical intervention criteria.

In recent years, there has been increased interest in machine learning (ML), a subset of artificial intelligence, for its promise for improving patient risk assessment(12). Many different ML algorithms have been investigated for a wide range of applications in cardiovascular disease, including the prediction of patient risk of complication and mortality (13–15). The use of a ML approach for risk assessment in TAA patients could provide an additional, more integrated metric for clinicians to consider when recommending intervention.

This study seeks to determine the feasibility and added value of using a ML approach to predict aortic biomechanical function from patient specific clinical data. The ex-vivo measured biomechanical metric of energy loss for healthy and aneurysmal patients was used as a representative output. The input variables to the model include information from an extensive database of pre-surgical clinical data, with factors including physical examination metrics, observations from medical imaging, family history, and genetic test results. The training process of this model reveals the relative significance and covarying trends of various clinical factors with energy loss. Additionally, the added benefit of integrated an echocardiography derived in-vivo stiffness metric as an input factor was assessed.

Methods

Study Cohort

In compliance with the Canadian tri-council policy statement on ethical conduct for research involving humans, informed consent was obtained from July 2012 to December 2021, from patients undergoing elective aortic valve or aortic resection surgery. Control aortic tissue was obtained from heart transplant donors and autopsy patients without heart or aortic disease.

A total of 158 patients were included in this study. Patient clinical information was collected during visits with a multidisciplinary aortopathy clinic at the McGill University Health Centre and retrospectively from patients' pre-surgical assessments (table 1). Potentially significant factors were selected based on the collaborative input of the members of the clinic.

Table 1: Considered clinical and echocardiographic variables

Input Variables	Variable Type	Input Options
Female	Logical	
Age (yr)	Numeric	
Height (m)	Numeric	
BSA (m^2)	Numeric	
BMI (kg/m^2)	Numeric	
Systolic Pressure (mmHg)	Categorical	0= 0-119, 1=120-129, 2=130-139, 3=140-179, 4= >180
Diastolic pressure (mmHg)	Categorical	0= 0-79, 1=80-89, 2=90-119, 3=>120
History of Hypertension (HTN)	Logical	
Diabetes (Type I/II) (DM)	Logical	
Dyslipidemia (DLP)	Logical	
Coronary Artery Disease (CAD)	Logical	
Heavy Weightlifting	Logical	
History of Smoking (Smoking)	Logical	
Regular Alcohol Consumption (EtOH)	Logical	
NYHA Heart Failure Symptoms	Logical	
Bicuspid Aortic Valve (BAV)	Logical	
AscAo Diameter (mm)	Logical	
SoV Diameter (mm)	Numeric	
AscAo diameter/BSA (mm/m^2)	Numeric	
Type II Aneurysm	Logical	
Family history (Fam HX)	Logical	
Clinical Featuring	Logical	
Marfan's Syndrome (MFN)	Categorical	0=none, 1= FBN1 VUS, 2=Positive
Other Positive Genetic Variant (PosVar)	Logical	
Variant of unknown significance (VUS)	Logical	
Aortic Stenosis (AS)	Categorical	0=none, 1=mild, 2=moderate, 3=severe
Aortic Regurgitation (AR)	Categorical	0=none, 1=mild, 2=moderate, 3=severe
CCPM (mmHg)	Numeric	

AscAo = Ascending aorta, CCPM = Cardiac cycle pressure modulus, SoV = Sinus of Valsalva, VUS = genetic variant of unknown significance

Genetic Paneling

A total of 37 patients were recommended for genetic testing by the aortopathy clinic. Genetic testing was performed using the Marfan's syndrome and Related Aortopathies Panel (Prevention Genetics, Marshfield, Wis), including 43 relevant aortopathy genes: ACTA2 (NM_001613.2), COL3A1 (NM_000090.3), FBN1 (NM_000138.4), FOXE3 (NM_012186.2), LOX (NM_002317.6), MAT2A (NM_005911.5), MFAP5 (NM_003480.3), MYH11 (NM_001040113.1), MYH11 (NM_001040114.1), MYLK (NM_053025.3), NOTCH1 (NM_017617.4), PRKG1 (NM_001098512.2), PRKG1 (NM_006258.3), SMAD3 (NM_005902.3), SMAD3 (NM_001145103.1), SMAD4 (NM_005359.5), TGFB2 (NM_003238.4), TGFB2 (NM_001135599.3), TGFB3 (NM_003239.4), TGFB3 (NM_001329938.1), TGFBR1 (NM_004612.3), TGFBR1 (NM_001306210.1), TGFBR2 (NM_003242.5), TGFBR2 (NM_001024847.2). A total of 3 syndromic patients had an outside diagnosis.

Aortic Geometries

Aortic geometries were determined from transesophageal echocardiographic (TEE) images performed at the time of surgery, after administered anesthetic but before the sternotomy, using a GE Vivid 7 echocardiographic unit (GE Healthcare, Madison, Wis). The TEE probe was inserted into the esophagus to the level of the ascending aorta (AscAo) where an ECG gated, 2-dimensional long axis view of the aortic valve and AscAo was captured, along with a 2-dimensional short-axis view at the point of maximum dilation. Diameter measurements at the Sinus of Valsalva and the mid AscAo were determined from the long axis view using the linear measurement tool in InteleViewer (4-14-1-P249; Intelerad, Montreal, QC). Aortic surface area

was measured from the short axis view, using the elliptical/circular ROI measurement tool in InteleViewer. Both measurements were taken at the R-interval of the ECG trace.

Ex-vivo Tensile Analysis

Testing was done within 24 hours of tissue collection, and the specimens were stored in physiologic saline at 4℃ until testing was completed. The aortic ring was clipped for orientation upon collection, and four 1.5cm by 1.5cm squared were sectioned, equally distributed around the circumference of the aorta. Five unique thickness measurements were taken for each testing square using a Mitutoyo Litematic VL-50A constant force digital micrometer (Mitutoyo Corp, Kanagawa, Japan). The testing squares were then connected to an EnduraTEC ELF 3200 planar biaxial tensile tester (Bose, Eden Prairie, Minn) using hooked 4-0 silk sutures in a 37℃ bath of Ringer's lactate solution. The testing squares were oriented for equiaxial stretching along their circumferential and longitudinal axes. Each sample was preconditioned for 7 cycles (ie, stretch and relaxation) followed by 3 cycles of data acquisition at a constant displacement rate of 0.1 mm/s in the range of 0% to 60% strain. The resultant stress-strain relations were analyzed using MATLAB (vR2021b;MathWorks, Natick, Mass). More detailed tensile methodology using this setup has been described previously(5, 16–18).

Energy loss of both axes was calculated from the engineering stress-strain relation. Energy loss is the percentage of elastic energy needed to stretch the testing square that is dissipated when the tissue is relaxed. The physiological interpretation is the percent of loss of elastic recoil energy in the tissue that is not returned to blood flow (ie, maintaining normal Windkessel function (19)).

The physical definition is the ratio of the area between the loading and unloading curve over the area under the loading curve, as shown in figure 1.

Transesophageal Echocardiographic Analysis

TEE-analysis was performed on patients from February 2016 to December 2021. When capturing the 2-dimensional short-axis view at the point of maximum dilation, an ECG gated strain cycle was captured for 3 heartbeats, ensuring 1 nontruncated cycle. In tandem, an invasive arterial pressure trace was taken from the patient's radial artery for the same measurement interval.

TEE speckle-tracking strain analysis was performed using GE's EchoPAC software (GE Healthcare). This analysis has been described in more detail previously (6).
Using the strain definition provided by Voigt et al. (20) for 2D speckle track echo ($\varepsilon = [\lambda - 1];\ \lambda = \mathrm{L}/\mathrm{L}_0$), radial strain ($\varepsilon_{Rad}$) was converted to radial stretch (λ_{Rad}). Second, the circumferential stretch (λ_{Circ}) profile was calculated using the conservation of volume: $\lambda_{Circ} = \sqrt{(1/\lambda_{Rad})}$, assuming stretching is both incompressible (21) and that circumferential and longitudinal stretching is equibiaxial (22, 23) in the physiological range. Cardiac Cycle Pressure Modulus (CCPM) as defined in Emmott et al. (6) was calculated as the slope of a linear interpolation of the radial blood pressure vs. the circumferential wall stretch (figure 1).

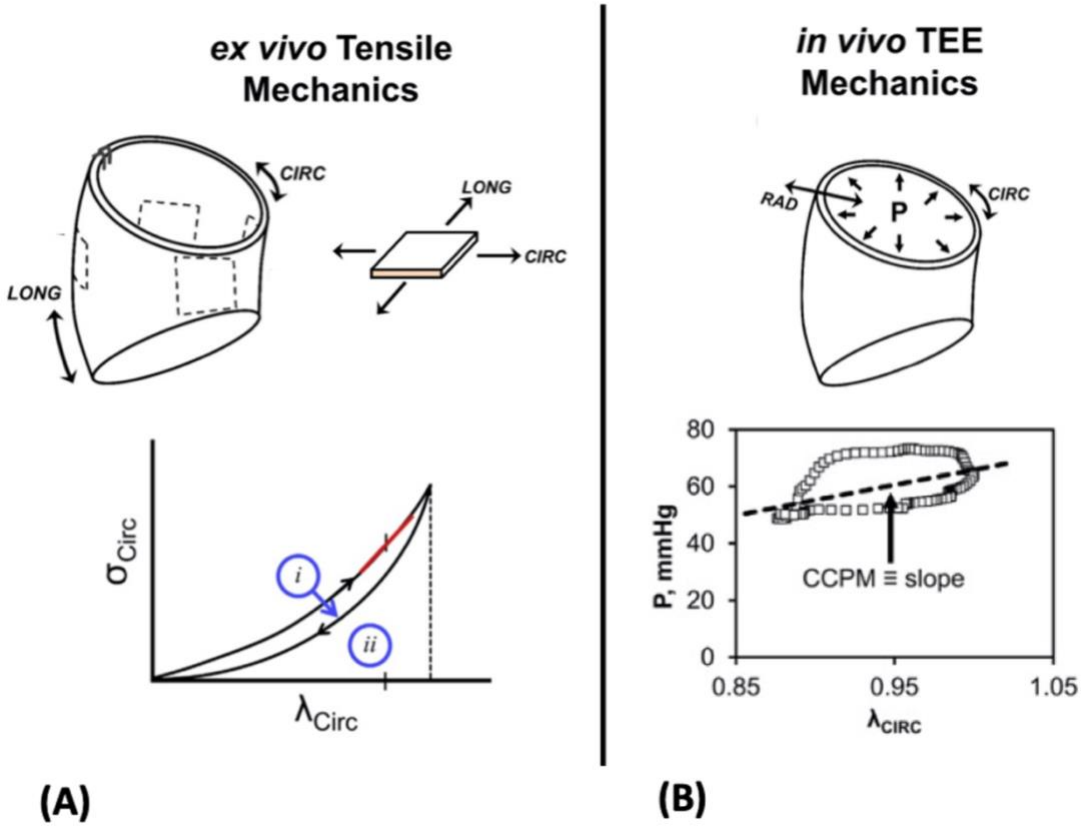

Figure 1: AscAo mechanics using ex-vivo tensile analysis and TEE-derived metric.

A) Four 1.5 x 1.5 cm2 testing squares were taken from around the circumference of the aortic ring. Specimens were stretched biaxially along the circumferential (Circ) and longitudinal (Long) axes to obtain the stress stretch profile. Energy loss is defined as the area between the loading and unloading curve divided by the area under the loading curve. Energy loss = Area(i) / [Area(i) + Area(ii)] x 100%. B) In-vivo, the aorta expands and recoils with changes in blood pressure. A transesophageal echocardiographic (TEE) speckle-track strain image of the radial (rad) strain was taken over 1 cardiac cycle and converted to circumferential (circ) stretch. Blood pressure-stretch curves were determined, with the slope of the linear fit being defined as the Cardiac cycle pressure modulus (CCPM) (as described by Emmott et al. (6)).

Machine Learning Analysis

Unsupervised and supervised ML algorithms were performed using MATLAB (vR2021b;MathWorks, Natick, Mass). Supervised models were trained in regression learner application from the Statistics and Machine Learning Toolbox.

Patients were split randomly in a 75:25 ratio to create training and testing data sets (119 and 39 patients, respectively). A t-test between all variables of the two datasets confirmed no significant differences in demographics. Energy loss was capped at 2 standard deviations above the population median, giving a maximum energy loss at 40%.

Supervised learning was performed considering four ML algorithms; linear regression, support vector matrix (SVM), random forest, and gaussian processes regression (GPR). Performance was quantified in terms of the R^2 and mean squared error (MSE) found by 5-fold cross validation of the training data. The presence of overfitting was assessed using the testing set, through the change in MSE relative to the training data. An increase in MSE greater than 10% was considered overfit.

Variable selection was conducted on the training data set (Figure 2). Initially an F-score ranking method was used, a univariate variable selection method that determines the relationship each variable has to the output on an independent basis. The interactive importance of the remaining variables was then determined through a wrapper method approach, as a second round of variable selection.

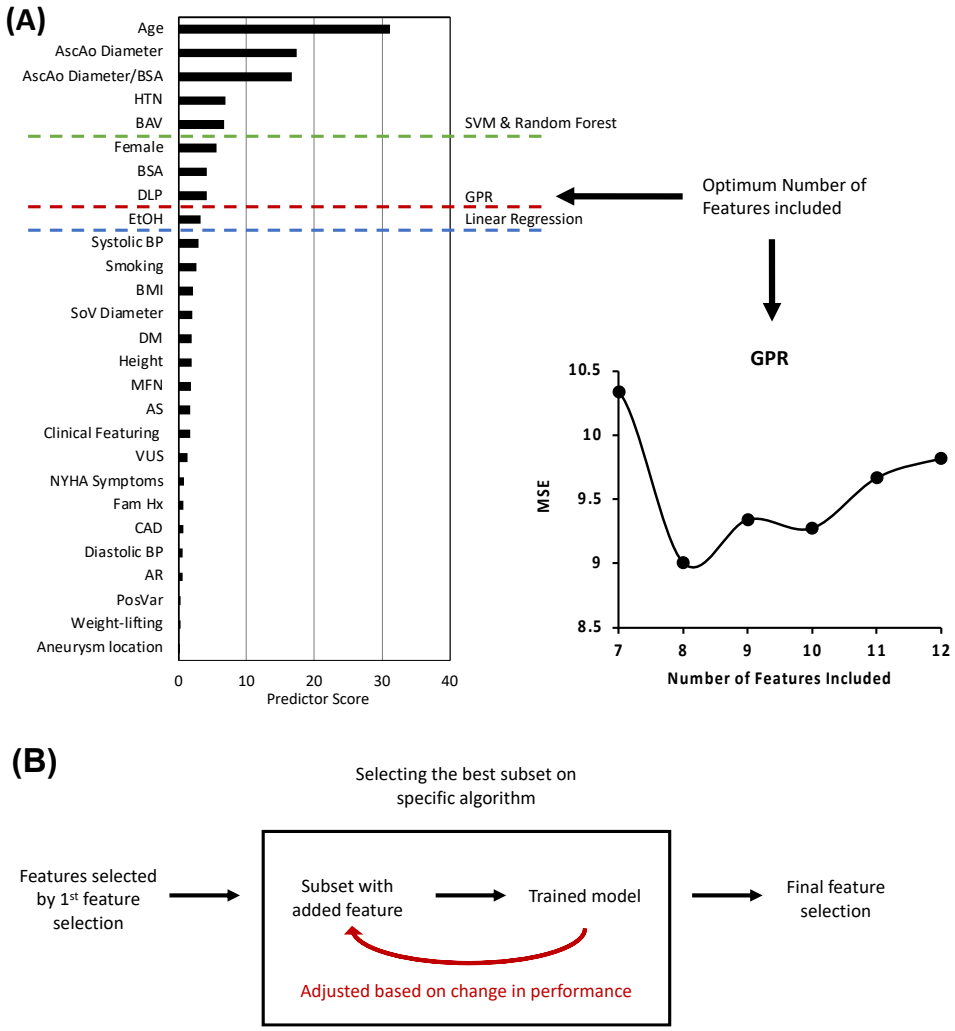

Figure 2: Two stage process for selecting significant clinical predictors.

A) An F-test was used to assign a predictor importance score for the relationship of each considered predictor with energy loss. Predictor importance = -log(p-value). The number of included variables for each model type was determined by MSE, exemplified with the GPR model type. Number of included features for each model type indicated with dotted line. B) A wrapper method used to consider the addition of the remaining features. A specific algorithm was retrained iteratively adjusting the subset of variables included to find an optimum based on minimum MSE. GPR = Gaussian process regression, MSE = Mean squared error, SVM = support vector machine.

A sub cohort of 67 patients had sufficient TEE images to perform the TEE analysis, with some patients discarded due to poor visualization of the aortic walls. Supervised learning was performed using the same variable selection and ML algorithms as the full cohort. All 67 patients were included for model training, with validation done by 5-fold cross validation.

Statistical Analysis

Statistical analyses were performed using GraphPad Prism, version 5.01 (GraphPad Software, Inc, San Diego, Calif). Correlations were calculated using linear regression. T-tests were performed by Welch's t-test for unequal variance. Prediction intervals are shown on plots with dashed black lines. Confidence intervals are shown on plots with dotted black lines. Results were considered significantly different when $P<0.05$.

Results

A total of 158 patients were recruited for the study, including 11 control patients (Table 2). Aneurysmal and control patients had mean ages of 63 ± 14 yr and 49 ± 16 yr ($P=0.02$), respectively, and mean AscAo diameters of 49 ± 8 mm and 25 ± 5 mm ($P<0.0001$). Of the included patients, a subset of 67 underwent TEE analysis. The TEE analysis cohort does not include control patients and had a similar mean age of 63 ± 14 yr and diameter 48 ± 9 mm to the original cohort.

Table 2: Baseline Characteristics of Cohort

Characteristic	Missing Data	Full Cohort (n=158)	TEE-Analysis Cohort (n=67)
Basic Patient Information			
Age (yr)	0	62 ± 14	63 ± 14
Female	0	22% (35)	22% (15)
Height (m)	<1%	1.7 ± 0.1	1.7 ± 0.1
BSA (m^2)	<1%	2.0 ± 0.2	2.0 ± 0.3
BMI (kg/m^2)	<1%	27 ± 5	27 ± 5
Disease Specifications			
Ascending Aortic (AscAo) Diameter (mm)	0	47 ± 10	48 ± 9
Sinus of Valsalva (SoV) Diameter (mm)	7%	40 ± 9	40 ± 9
Aneurysm Location	<1%		
AscAo		65% (103)	70% (47)
Sov		28% (44)	30% (20)
Non-Aneurysmal		7% (11)	0% (0)
Bicuspid Aortic Valve (BAV)	0	46% (73)	49% (33)
NYHA Symptoms	11%	53% (84)	54% (36)
Aortic stenosis (AS)	0		
Mild		9% (15)	7% (5)
Mod		6% (9)	4% (3)
Severe		28% (45)	34% (23)
Aortic Regurgitation (AR)	0		
Mild		22% (34)	22% (15)
Mod		22% (35)	24% (16)
Severe		17% (27)	18% (12)
Comorbidities			
History of Hypertension (HTN)	0	54% (85)	52% (35)
Diabetes (Type I/II) (DM)	0	11% (18)	12% (8)
Dyslipidemia (DLP)	0	26% (41)	24% (16)
Coronary Artery Disease (CAD)	0	21% (33)	16% (11)
Life-Style Factors			
Heavy weightlifting	0	3% (5)	4% (3)
History of smoking (Smoking)	3%	16% (25)	7% (5)
Regular Alcohol Consumption (EtOH)	3%	14% (22)	22% (15)
Genetic Information			
Family history (Fam Hx)	37%	26% (41)	24% (16)
Clinical Featuring	0	7% (11)	9% (6)
Genetic testing done	0	25% (40)	36% (24)
Marfan's Syndrome (MFS)	0	3% (5)	3% (2)
Other Positive Genetic Variant (PosVar)	0	3% (5)	7% (5)
Variant of unknown significance (VUS)	0	7% (11)	10% (7)

[a]Values are mean ± SD or % (n)

From the full cohort, the aneurysmal patients had a mean energy loss of 31±5%, which was significantly greater than the mean energy loss for the healthy control patients 26±3% (P=0.0001) (figure 3). This is consistent with previous findings (5). With respect to the clinical markers of the patients, energy loss correlates significantly with patient age, R^2=0.38, P<0.0001, and with AscAo diameter, R^2=0.26, P<0.0001, both with a positive correlation.

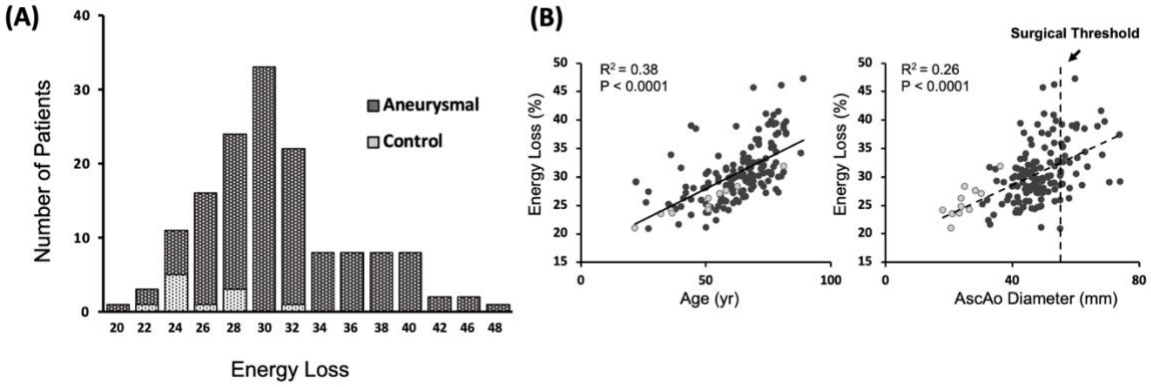

Figure 3: Overview of measured energy loss for study cohort.

A) Overlapping histogram of measured energy loss values for aneurysmal and control patients.

B) Scatter plots comparing ex-vivo measures of energy loss to common clinical metrics. (Left) Patient age at the time of surgery. (Right) In-vivo measured ascending aortic diameter. Surgical diameter threshold indicated at 55 mm.

The energy loss increases with aortic diameter >55 mm. The average energy loss in aortas <55 mm and >55 mm is 30%±5% and 34%±5%, respectively (P=0.0002). At the level of the surgical threshold diameter, the measured energy loss values range from a healthy physiological range at 21% to the high end of the population at 39%.

Predictive Model from Clinical Data:

Variables selected by f-test ranking for each of the four ML algorithms are indicated in figure 2a, with SVM and random forest having optimal performance with 5 variables, GPR with 8, and linear regression with 9. The final variables selected after wrapper method are provided in table 3. The GPR based model was found to have the greatest performance compared to the other ML models. A total of 13 variables were included, giving R^2=0.63 and MSE=8.69, with no significant reduction in performance with the external testing set.

Currently accepted clinical metrics, such as diameter indexed to patient BSA, and aortic surface area indexed to patient height were also assessed for their correlative relationship with energy loss. For a direct comparison with the models, linear regressions were created for each of these metrics using the training data set, and correlation was represented in terms of cross validation, and external testing set. A multi linear regression of patient age and AscAo diameter was also considered.

Table 3: Summary of Model Performance with Full Cohort

Model Type (n of variables)	Included Variables	CV R^2	CV MSE	Testing MSE
Machine Learning Models				
LINEAR REGRESSION (10)	Age, AscAo diameter, AscAo diameter/BSA, HTN, BAV, Female, BSA, DLP, EtOH, Aneurysm type	0.62	9.27	9.78
SUPPORT VECTOR MACHINE (8)	Age, AscAo diameter, AscAo diameter/BSA, HTN, BAV, BSA, EtOH, VUS	0.60	9.56	9.97
RANDOM FOREST (5)	Age, AscAo diameter, AscAo diameter/BSA, HTN, BAV	0.55	10.7	9.63
GAUSSIAN PROCESS REGRESSION (13)	Age, AscAo diameter, AscAo diameter/BSA, HTN, BAV, Female, BSA, DLP, SoV Diameter, Type II Aneurysm, AS, Marfan, Heavy weightlifting	0.63	8.69	8.78
Diagnostic Metrics				
LINEAR REGRESSION (1)	AscAo Diameter	0.26	17.5	15.7
	AscAo Diameter/BSA	0.32	16.3	13.5
	AscAo Surface Area/Height	0.29	16.8	15.9
LINEAR REGRESSION (2)	Age, AscAo Diameter	0.51	11.4	10.7

AscAo = Ascending aorta, BAV = Bicuspid aortic valve, BSA = Body surface area, CV = 5-fold cross validation, DLP = Dyslipidemia, HTN = Hypertension, MSE = mean squared error, SoV = Sinus of Valsalva, VUS = variant of unknown significance

The correlative performance of the considered diagnostic metrics, AscAo diameter, AscAo diameter/BSA, and AscAo surface area/height, were found to be surprisingly low, with R^2 values of 0.26, 0.32, and 0.29, respectively. A multi linear regression of patient age and diameter was found to have a significant improvement with R^2=0.51, still being considerably lower than any of the ML models.

A performance plot of the resultant GPR based model shows that 90% (107 of 119) of the predicted data points fall within a 95% prediction interval of the data (Figure 4). Most of the prediction outliers (6 of 12) occurring at the highest end of the curve, at energy loss values

>35%, with the predicted values being less than those that were measured. There is no significant difference in prediction error between the tricuspid (TAV) and bicuspid valve (BAV) patients (TAV MSE=5.48, BAV MSE=5.19, P=0.85).

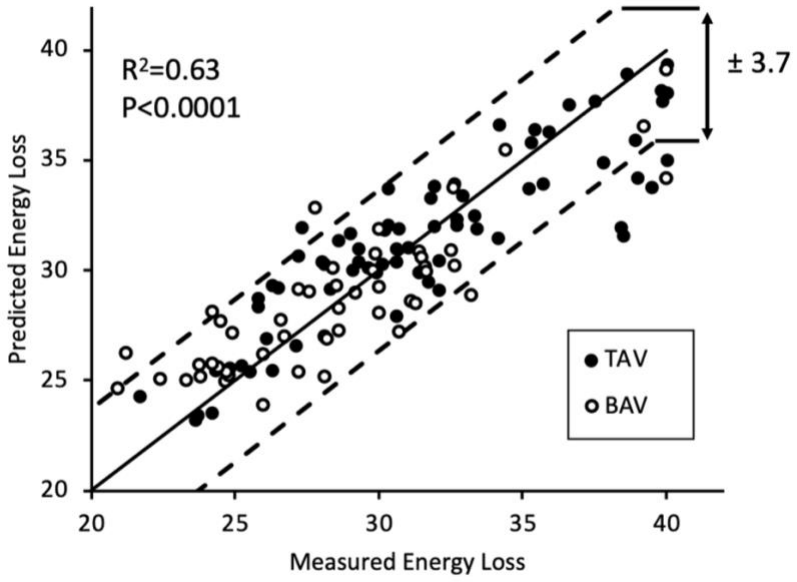

Figure 4: Predictive performance of GPR model trained on full cohort.

Predicted values shown for training data set, with indicated R2 found by 5-fold cross validation. Solid black line indicates line of perfect prediction at y=x. Dotted lines represent 95% prediction interval, with a total width of 7.3-7.4%. BAV = Bicuspid aortic valve, GPR = Gaussian process regression, TAV = Tricuspid aortic valve

Predictive Model with TEE derived Stiffness:

Each ML algorithm was retrained, using the same variable selection determined in the previous section, on the TEE analysis cohort (table 4). The CCPM modulus was added as an additional variable. The addition of the CCPM gave at least a 20% reduction in MSE for all considered ML models. The best performing model for this data set was found again to be the GPR based model,

with an R^2=0.62 and MSE=8.60, noting that the performance of the original model discussed in the previous section was decreased from the R^2=0.63 found using the full cohort, to an R^2=0.46 with the significantly smaller TEE cohort. Once again, for a direct comparison with the models, a linear regression of CCPM was trained, having an R^2=0.53 and MSE=10.6 by cross validation.

Table 4: Summary of Model Performance with TEE-analysis Cohort

Model Type	CV R^2	CV MSE
ML Models		
LINEAR REGRESSION	0.47	11.6
SVM	0.37	14.1
RANDOM FOREST	0.44	12.2
GPR	0.46	12.0
ML Models with CCPM		
LINEAR REGRESSION	0.57	9.31
SVM	0.52	10.8
RANDOM FOREST	0.57	9.28
GPR	0.62	8.60
Diagnostic Metrics		
CCPM[a]	0.53	10.6

[a]Linear regression of CCPM

CCPM = cardiac cycle pressure modulus, CV = 5-fold Cross validation, GPR = gaussian process regression, ML = machine learning, MSE = mean squared error, SVM = support vector machine

Performance plots for the linear regression of CCPM, the original GPR model, and combined GPR model with CCPM are shown (figure 5). With respect to the 95% prediction interval, the CCPM based model shows 34% of its predictions (23 out of 67 patients) as outliers, with an even distribution of high and low predictions along the entire x-axis. The original GPR model has 16% (11 out of 67) outliers, once again being concentrated at the high end of the curve (energy

loss >35%). With the combined approach the number of outliers from the prediction interval is reduced to 7% of patients (5 of 67).

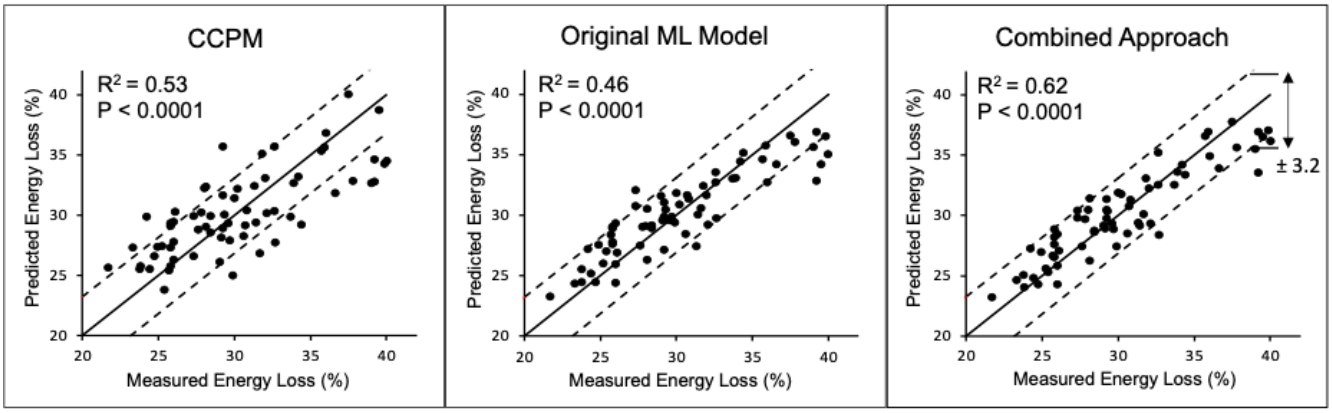

Figure 5: Comparison of prediction performance of considering clinical predictors and CCPM. Performance plots for (left) linear regression model trained on CCPM as only predictor, (middle) GPR model trained on 13 clinical predictors, and (right) GPR model trained on clinical predictors and CCPM. R2 values based on 5-fold cross validation. Solid black line indicating line of perfect prediction, 95% prediction interval shown with dotted line, having a total width of 6.2-6.4%. CCPM = cardiac cycle pressure modulus, GPR = gaussian process regression

Discussion

A ML approach was used to predict the biomechanical function of human TAA tissue from patient specific clinical data. Energy loss was used as the representative output for this analysis as it is a highly robust and self-normalizing metric, that has been demonstrated to correlate with the degree of medial degeneration in aneurysmal tissue (5). A regression-based ML model was found to have a much greater correlative measure with energy loss than simpler size-based metrics on their own. Compared to the surprisingly poor correlation of AscAo diameter with

energy loss, (R^2=0.26, MSE=17.5), a GPR based model including 13 clinical variables has an improvement in MSE of up to 67% (R^2=0.63, MSE=8.69). Even when considering a multilinear regression of patient age and diameter (R^2=0.51, MSE=11.4), there is a significant improvement with the ML model, justifying the added benefit of considering a broader range of patient information. The most significant variables with respect to energy loss were patient age and AscAo diameter, however, both genetic and traditional cardiac risk factors were shown to have a positive influence on prediction as well. This method was improved further with the addition of a medical imaging derived stiffness metric, CCPM, as an input variable.

The results of the f-test ranking of variable importance reveals that patient age, by far, has the strongest relationship to energy loss. Meaning the effect of the aorta's natural remodeling and stiffening with age is responsible for the largest amount of variation within this patient population. A recent study by Durbak et al found similar evidence that age is the most influential factor in elastic energy storage in the thoracic aorta (11), with other studies finding similar relationships between age and other mechanical testing indexes in both diseased (24) and healthy tissue (25). As such, this factor needs to be considered in the clinical interpretation of the predicted energy loss value (figure 6).

Once made, energy loss predictions can be considered with respect to the population average for their age group. Levels of predicted risk can then be assigned with respect to deviation from the population mean. This is exemplified by two patients of a similar age group, shown as (i) and (ii) in figure 6. Both patients present as having degenerative aortopathy, at 71 and 69 years old, and both have low prediction error (<1%). Patient (i) presents with a mildly dilated aorta of

46mm, below the surgical cut-off, however, the energy loss is predicted at 36%. With respect to the population mean for this respective age level, this prediction was found to be above average. Clinically, this patient can then be flagged as potentially being at higher risk. Comparatively, patient (ii) presents with similar diameter, age and comorbidities, but has a predicted energy loss much lower, at 29%, below the population average, justifying that they are not expected to be at immediate risk.

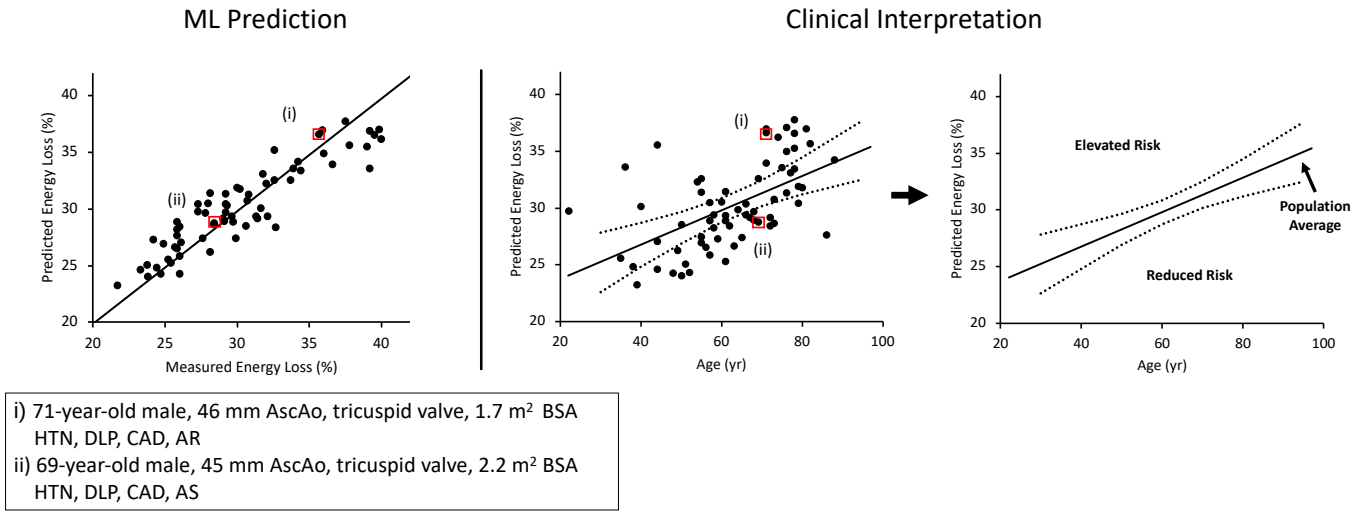

Figure 6: Clinical interpretation of model predictions by indexing with patient age. (Left) Energy loss predictions are made using the gaussian process regression model trained on TEE-analysis cohort with CCPM included. (Right) These predicted energy loss values can be represented as a function of patient age at the time of surgery. Linear regression line representing population average, dotted line showing 99% confidence interval, providing an example of risk category thresholds. Example patients (i) and (ii) are indicated by red square. AR = Aortic regurgitation, AS = aortic stenosis, CAD = coronary artery disease, CCPM = cardiac cycle pressure modulus, DLP = dyslipidemia, HTN = hypertension

The further development of this method would be clinically useful as a decision support system. Particularly in low resource centers, where a model of this type can be used as a screening method for recommending patients to be considered more closely by a specialist. This approach can be easily integrated into the clinical environment as a desktop application in which patient data is inputted within the clinic, immediately generating the predicted risk.

When considering the clinical factors that were selected as significant, a diagnosis of Marfan is the only genetic test result that was found to improve the performance of the GPR model. This is likely because this test result has the largest number of patients included (n=5), while the positive genetic variants and variants of unknown significant have an incidence of n=1 with respect to their affected genes. Similarly, hypertension and dyslipidemia are the two comorbidities determined to have a positive affect for the model, being the two most common comorbidities within the patient population. Presumably with a larger patient cohort, trends relating to less common comorbidities or genetic variants can be better represented.

From the performance plot of the models (figure 4), in the high energy loss region (>35%), it can be suggested that with extreme high levels of disease progression, mechanical function may be more heavily influenced by another driving force that is not being adequately represented by the considered factors. The lack of information of the growth rate of the aneurysm is potentially the missing piece in this problem. With the high rate of incidental findings in TAA patients, the rate of growth is unknown in most cases. Growth rate is known to be an important indicator the risk and has been speculated to correspond to different driving forces of medial degeneration (2, 9, 26).

The integration of CCPM into the model likely makes up for this lack of information. The metric CCPM on its own has the advantage of being directly related to the function of the aortic tissue at the time of surgery. However, the complexity of the image, and lack in robustness of stiffness on its own makes its correlative power to energy loss limited. Resultantly, the combination of the two methods gives a greater prediction of energy loss than either individual method produces on its own.

The relative success of this method, compared to the currently considered methods of diameter-based thresholds and echocardiographic derived stiffness metrics, justifies the validity of this approach. The addition of more patients to the study cohort will help to further refine the model and narrow the prediction intervals of the correlation. Overall, these findings heavily support the conclusion that a larger scope study of this nature should be considered.

Limitations

The largest limitation of this study is the use of energy loss as a surrogate for risk of aortic complication. There is inherently a strong relationship between biomechanical function and patient's risk of complication, however, the heterogeneity within the patient population makes the use of any single metric to represent risk unrealistic. Incidents of dissection and rupture are highly localized phenomenon within the aorta, which cannot be accounted for with a single average value of the entire tissue segment. The ideal approach would be to follow a large cohort, using their incidence of complications as the representative outputs to a ML model. However, doing so would require withholding intervention from potentially at-risk patients.

It should also be noted that socioeconomic data is not considered by this study. It is becoming increasingly evident that economic class plays a significant role in a patients access to care, and likely risk factors. With the burden of cardiovascular disease being increased in low-resource settings (27, 28). Additionally, given the location of this study, the patient cohort is heavily made of up of Caucasian patients, with patients of other races being disproportionately underrepresented. Therefore, these findings cannot be assumed to be applicable to all demographics.

Conclusions

This ML analysis demonstrates that using an approach that integrates various clinical metrics does provide a more accurate prediction of aortic mechanical function than simpler size-based metrics currently adopted by the field. Preliminary models were able to incorporate common traditional cardiac risk factors such as comorbidities and Marfan's syndrome. The limitations in prediction by this approach highlight the heterogeneous and complex nature of this disease, however, these limitations can be addressed with a combined approach using TEE speckle tracking derived metrics as addition inputs to the model.

Overall, this study indicates the relative success of this method compared to those which are currently used. This provides support for the collection of mechanical data of this nature on a larger scale in the pursuit or creating an in-vivo prediction of energy loss for clinical decision-making support.

References

1. Booher AM, Eagle KA. Diagnosis and management issues in thoracic aortic aneurysm. American Heart Journal 2011;162:38-46.e1.

2. Hiratzka LF, Bakris GL, Beckman JA, et al. 2010 ACCF/AHA/AATS/ACR/ASA/SCA/SCAI/SIR/STS/SVM Guidelines for the Diagnosis and Management of Patients With Thoracic Aortic Disease. Circulation 2010;121.

3. Boodhwani M, Andelfinger G, Leipsic J, et al. Canadian Cardiovascular Society Position Statement on the Management of Thoracic Aortic Disease. Canadian Journal of Cardiology 2014;30:577–589.

4. Pape LA, Tsai TT, Isselbacher EM, et al. Aortic Diameter ≥5.5 cm Is Not a Good Predictor of Type A Aortic Dissection. Circulation 2007;116:1120–1127.

5. Chung J, Lachapelle K, Wener E, et al. Energy loss, a novel biomechanical parameter, correlates with aortic aneurysm size and histopathologic findings. The Journal of Thoracic and Cardiovascular Surgery 2014;148:1082–1089.

6. Emmott A, Alzahrani H, Alreshidan M, Therrien J, Leask RL, Lachapelle K. Transesophageal echocardiographic strain imaging predicts aortic biomechanics: Beyond diameter. The Journal of Thoracic and Cardiovascular Surgery 2018;156:503-512.e1.

7. Baumgartner D, Baumgartner C, Mátyás G, et al. Diagnostic power of aortic elastic properties in young patients with Marfan syndrome. The Journal of Thoracic and Cardiovascular Surgery 2005;129:730–739.

8. Vitarelli A, Giordano M, Germano G, et al. Assessment of ascending aorta wall stiffness in hypertensive patients by tissue Doppler imaging and strain Doppler echocardiography. Heart 2010;96:1469–1474.

9. Cheung K, Boodhwani M, Chan K, Beauchesne L, Dick A, Coutinho T. Thoracic Aortic Aneurysm Growth: Role of Sex and Aneurysm Etiology. J Am Heart Assoc 2017;6.

10. Collins JA, Munoz J-V, Patel TR, Loukas M, Tubbs RS. The anatomy of the aging aorta. Clinical Anatomy 2014;27:463–466.

11. Durbak E, Tarraf S, Gillespie C, et al. Ex vivo biaxial load testing analysis of aortic biomechanics demonstrates variation in elastic energy distribution across the aortic zone zero. The Journal of Thoracic and Cardiovascular Surgery 2021.

12. Cuocolo R, Perillo T, de Rosa E, Ugga L, Petretta M. Current applications of big data and machine learning in cardiology. J Geriatr Cardiol 2019;16:601–607.

13. Motwani M, Dey D, Berman DS, et al. Machine learning for prediction of all-cause mortality in patients with suspected coronary artery disease: a 5-year multicentre prospective registry analysis. European Heart Journal 2016:ehw188.

14. Sánchez-Cabo F, Rossello X, Fuster V, et al. Machine Learning Improves Cardiovascular Risk Definition for Young, Asymptomatic Individuals. J Am Coll Cardiol 2020;76:1674–1685.

15. Miranda E, Irwansyah E, Amelga AY, Maribondang MM, Salim M. Detection of Cardiovascular Disease Risk's Level for Adults Using Naive Bayes Classifier. Healthcare Informatics Research 2016;22:196.

16. Choudhury N, Bouchot O, Rouleau L, et al. Local mechanical and structural properties of healthy and diseased human ascending aorta tissue. Cardiovascular Pathology 2009;18:83–91.

17. Tremblay D, Cartier R, Mongrain R, Leask RL. Regional dependency of the vascular smooth muscle cell contribution to the mechanical properties of the pig ascending aortic tissue. Journal of Biomechanics 2010;43:2448–2451.

18. Tremblay D, Leask RL. Remodelling and pathology development associated with aneurysmal ascending aortic tissues. The Canadian Journal of Chemical Engineering 2011;89:13–22.

19. Belz GG. Elastic properties and Windkessel function of the human aorta. Cardiovascular Drugs and Therapy 1995;9:73–83.

20. Voigt J-U, Pedrizzetti G, Lysyansky P, et al. Definitions for a Common Standard for 2D Speckle Tracking Echocardiography: Consensus Document of the EACVI/ASE/Industry Task Force to Standardize Deformation Imaging. Journal of the American Society of Echocardiography 2015;28:183–193.

21. CAREW TE, VAISHNAV RN, PATEL DJ. Compressibility of the Arterial Wall. Circulation Research 1968;23:61–68.

22. Bell V, Mitchell WA, Sigurðsson S, et al. Longitudinal and Circumferential Strain of the Proximal Aorta. J Am Heart Assoc 2014;3.

23. Wittek A, Karatolios K, Fritzen C-P, et al. Cyclic three-dimensional wall motion of the human ascending and abdominal aorta characterized by time-resolved three-dimensional ultrasound speckle tracking. Biomechanics and Modeling in Mechanobiology 2016;15:1375–1388.

24. Okamoto RJ, Xu H, Kouchoukos NT, Moon MR, Sundt TM. The influence of mechanical properties on wall stress and distensibility of the dilated ascending aorta. The Journal of Thoracic and Cardiovascular Surgery 2003;126:842–850.

25. Guinea G v, Atienza JM, Rojo FJ, et al. Factors influencing the mechanical behaviour of healthy human descending thoracic aorta. Physiological Measurement 2010;31:1553–1565.

26. Masuda Y, Takanashi K, Takasu J, Morooka N, Inagaki Y. Expansion Rate of Thoracic Aortic Aneurysms and Influencing Factors. Chest 1992;102:461–466.

27. Zhao Y, Wood EP, Mirin N, Cook SH, Chunara R. Social Determinants in Machine Learning Cardiovascular Disease Prediction Models: A Systematic Review. American Journal of Preventive Medicine 2021;61:596–605.

28. Ishwaran H, O'Brien R. Commentary: The problem of class imbalance in biomedical data. The Journal of Thoracic and Cardiovascular Surgery 2021;161:1940–1941.

Supplemental Appendix

Supplemental Methods

Treatment of Missing Data:

For the treatment of missing data, the clinical input features were divided into groups of relevancies as described in supplemental table 1. Only variables which were deemed to not be reasonably assumed were considered missing information for a given patients. Patients having greater than 25% missing data were removed from the study. Numerical values were filled in with the average of the data set, while categorical features were filled in with the least severe option.

Control patients for this study had known aortic geometries, and 5 of the 11 had a known age. All other features were assumed, as indicted in table 1. Patients with a missing age were estimated through a linear interpolation with the energy loss.

Supplemental Table 1: Treatment of missing data on all considered predictors

Input Features	Data Type	Treatment
Female	Logical	0[a]
Age (yr)	Numeric	Average [a]
Height (m)	Numeric	Average [a]
BSA (m^2)	Numeric	Average
BMI (kg/m^2)	Numeric	Average
Systolic Pressure (mmHg)	Categorical	1 [a]
Diastolic pressure (mmHg)	Categorical	1 [a]
History of Hypertension (HTN)	Logical	0 [b]
Diabetes (Type I/II) (DM)	Logical	0 [b]
Dyslipidemia (DLP)	Logical	0 [b]
Coronary Artery Disease (CAD)	Logical	0 [b]
Heavy Weightlifting	Logical	0 [b]
Clinical Featuring	Logical	0 [b]
NYHA Symptoms	Logical	0 [a]
History of Smoking (Smoking)	Logical	0 [a]
Regular Alcohol Consumption (EtOH)	Logical	0 [a]
Bicuspid Aortic Valve (BAV)	Logical	0 [a]
Ascending Aortic (AscAo) Diameter (mm)	Numeric	None [c]
Sinus of Valsalva (SoV) Diameter (mm)	Numeric	Average [a]
AscAo diameter/BSA (mm/m^2)	Numeric	
Type II Aneurysm	Logical	0 [a]
Family history (Fam HX)	Logical	0 [a]
Marfan's Syndrome (MFN)	Categorical	0 [b]
Other Positive Genetic Variant (PosVar)	Logical	0 [b]
Variant of unknown significance (VUS)	Logical	0 [b]
Aortic Stenosis (AS)	Categorical	0 [b]
Aortic Regurgitation (AR)	Categorical	0 [b]
Cardiac Cycle Pressure Modulus (CCPM)	Numeric	None [c]

[a]If not explicitely stated in-patient assessment considered to be missing information for that patient entry. Up to 25% of missing information allowed before removal from cohort. [b]If not stated in patient assessment can be reasonably assumed to be false, not considered to be missing information. [c]If information cannot be determined patient removed from dataset.

Machine Learning Alorithms:

In this analysis, 4 different regression-based machine learning model types were considered, linear regression, support vector machine, random forest, and gaussian process regression.

Linear Regression: Linear regression models are fit based on a least squares approach, to find the coefficients for each predicted which give the lowest overall error in the residuals.

The general equation for multi-linear regression is as follows:

$$y_i = \beta_0 + \beta_1 X_{i1} + \beta_2 X_{i2} + \cdots \beta_p X_{ip} \;\; i = 1, \ldots, n$$

y_i: is the predicted output for a given patient (i)

X_{ij}: is the observation for a given input variable (j), for a given patient (i)

β_j: is the coefficient for a given variable (j). β_0 is a constant term for the model.

Support Vector Machine: SVM fits a line with an allowable sensitivity region surrounding it, ε, creating a hyperplane through the data. SVM models try to fit the best line through the data, such that the most datapoints possible are within the hyperplane. Only the residuals of points that fall outside of the sensitivity threshold (Slack variables: ξ_i and ξ_i^*) are considered for minimization. Therefore, this method seeks to find a solution which minimizes the size of the hyperplane and the sum of the slack variables, according to the equation (1):

$$\frac{1}{2}\|w\|^2 + C\sum_{i=1}^{n}(\xi_i + \xi_i^*) \rightarrow min$$

Where C is the box constraint, a constant value set to act as the penalty on the slack variables to help prevent overfitting. The term w is the minimum normal solution for the coefficients in the training data set.

Supplemental Table 2: Model Parameters for SVM Model Type

Hyperparameter	Value
Kernel Function	Linear
Box Constraint (C)	4.5695
Epsilon (ε)	0.4569
Standardize Data	True

Gaussian Process Regression: This method treats each data point as a random sample in a p-dimensional gaussian distribution. For each data point a function is created out of the p-predictor responses. Once a function has been created for every patient, the model creates a probability distribution of these functions. When prediction is being made on a new point, the value is inferred using a Bayesian approach based on the previous observations. This is a non-parametric method, in that, as new data points are added, the method is iteratively computing and adapting the probability distribution of the possible functions (2). This has the advantage of being affecting with smaller datasets.

The covariance function, or kernel function of the model describes the assumptions being made about the form of the functions being modelled. The kernel function is used to determine how the value of one predictor affects another. For the case of this project, a squared exponential kernel function will be used. If the terms x_i and x_j are both n-by-1 matrixes, each representing the values of a given predictor, the following expression can be used to relate them (2):

$$k(x_i, x_j|\theta) = \sigma_f^2 \exp\left[-\frac{1}{2}\frac{(x_i - x_j)^T (x_i - x_j)}{\sigma_l^2}\right]$$

Where:

$k(x_i, x_j|\theta)$: Covariance function parameterized in terms of the kernel parameters θ

σ_l=Characteristic length scale

σ_f= Signal standard deviation

Supplemental Table 3: Model Parameters for GPR Model Type

Hyperparameter	Value
Basis Function	Constant
Kernel Function	Squared Exponential
Standardize	True
Characteristic Length Scale (σ_l)	5.3846
Signal Standard Deviation (σ_f)	6.0015

Random Forest: A regression tree ensemble is a model composed of a weighted combination of multiple regression trees. A regression tree divides the dataset into smaller groups based on threshold for the given predictors. Thresholds are determined using a least squares method. The groups of subdivided datapoints falls into bins, representing different outcomes, called leaves. In a regression tree, each leaf represents a numeric value for a response, being the average value of the datapoints assigned to the leaf.

In random forest regression trees were combined using bagging, which involves independently learning several regression trees in parallel, taking a random subset of the original data set for each. A random subset of the available predicted are sampled at each learning stage. The

predicted response for each individual regression tree are determined and an average between them is taken (3).

Supplemental Table 4: Model Parameters for Random Forest Model Type

Hyperparameter	Value
Ensemble Method	Bagging
Minimum Patients per Leaf	8
Number of Regression Trees	30
Number of predictors sampled per learning stage	2

Model Validation:

Model performance is quantified by two metrics; coefficient of determination (R^2) and mean squared error (MSE). Calculated by the following:

$$R^2 = 1 - \frac{\sum_i (y_i - \hat{y}_i)^2}{\sum_i (y_i - \bar{y}_i)^2}$$

y_i: predicted energy loss values (%)

$\hat{y}_i$: measured energy loss values (%)

$\bar{y}_i$: average predicted energy loss (%)

$$MSE = \frac{1}{n}\sum_{i=1}^{n} (y_i - \hat{y}_i)^2$$

Model validation was performed in two stages. During the pretreatment of the data, the dataset was divided in a 75:25 split to form two separate training and testing sets. Models were initially validated using the training dataset by cross validation. The dataset was then validated externally using the testing data set.

Cross validation is a method of validating a model while also using all the available data to train it. The training data is divided into k-folds, for the purposes of this analysis 5-folds were used. The model is then trained 5 separate times, each time leaving out one of the folds as the validation fold. After each iteration of training, new predictions are made for the data in the validation fold, and the R^2 and MSE of these predictions is calculated. Once all 5 training iterations are complete, the average R^2 and MSE is found (4). A final version of the model is then trained using all the folds for training. This method allows for an estimate of what the error would be on new testing data, while also using all the available data to train the model (5).

The external testing dataset was used once a model had been trained to determine its generalizability, and to assess if the model is overfit to the variance in the training data. The trained model was used to make predications on the new data, and the R^2 and MSE of these predictions is calculated. These metrics can be compared to that found by cross validation, if MSE is much higher in the testing set then this means the model is overfit to the training set, and therefore % Overfit will be a positive number >10%. Percentage overfit can be defined as:

$$\%\ Overfit = \left(1 - \frac{MSE_{CV}}{MSE_{testing}}\right) \times 100\%$$

MSE_{CV}: Mean squared error based on cross validation of training data set

$MSE_{testing}$: Mean squared error based on predictions made for testing data set

F-test Based Feature Selection:

An F-test was performed to rank the relative importance of each individual feature to the desired output. The hypothesis that when the response values are put into groups based on the predictor

values, they are drawn from populations with the same mean was testing. A small p-value for the test indicated that the corresponding predictor is important. The predictor importance scores are the -log (p-value). For numeric type variables, the algorithm automatically bins the variable. This was performed using the fsrftest function in MATLAB (vR2021b;MathWorks, Natick, Mass).

Wrapper Based Feature Selection:

The feature selection process for wrapper method is specific to the machine learning algorithm being trained. This method evaluates all possible combinations of features against an evaluation criterion. The criteria used to assess model performance was the MSE as determined by 5-fold cross validation.

In this case, this method begins with a model having only the features selected by f-test, and then each of the remaining available features were individually added. The added feature that creates the model with the lowest MSE was selected to be added. This process was repeated until all available features has been selected. As a result, the order of importance of the remaining features to the specific model type was determined. Models were then trained in the regression learner app to determine the number of added features giving the minimum MSE without being overfit to the training data.

This was performed in MATLAB using the sequentialfs function, specifying that the f-test selected features were to by kept, using the "keepin" command. The input "nfeatures" was specified as "all".

Gaussian Process Regression Model MATLAB Training Script

```
function [trainedModel, validationMSE] = trainRegressionModel (trainingData)
% [trainedModel, validationMSE] = trainRegressionModel (trainingData)
% Returns a trained regression model and its MSE. This code recreates the
% model trained in Regression Learner app. Use the generated code to
% automate training the same model with new data, or to learn how to
% programmatically train models.
%
% Input:
%  trainingData: A table containing the same predictor and response
%  columns as those imported into the app.
%
% Output:
%  trainedModel: A struct containing the trained regression model. The
%  struct contains various fields with information about the trained
%  model.
%
%  trainedModel.predictFcn: A function to make predictions on new data.
%
%  validationMSE: A double containing the MSE. In the app, the Models
%  pane displays the MSE for each model.
%
% Use the code to train the model with new data. To retrain your model,
% call the function from the command line with your original data or new
% data as the input argument trainingData.
%
% For example, to retrain a regression model trained with the original data
% set T, enter:
% [trainedModel, validationRMSE] = trainRegressionModel (T)
%
% To make predictions with the returned 'trainedModel' on new data T2, use
% yfit = trainedModel.predictFcn (T2)
%
% T2 must be a table containing at least the same predictor columns as used
% during training. For details, enter:
% trainedModel.HowToPredict
```

```
% Auto-generated by MATLAB on 01-Jun-2022 15:51:59


% Extract predictors and response
% This code processes the data into the right shape for training the
% model.
inputTable = trainingData;
predictorNames = {'Female', 'age', 'bsa', 'HTN', 'DLP', 'WeightLifter', 'BAV', 'AscAo D', 'SoV D', 'AscAoD_BSA',
'Type II Aneurysm', 'MFS', 'AS'};
predictors = inputTable (:, predictorNames);
response = inputTable.EnergyLossMeanmeanOfBothAxis;
isCategoricalPredictor = [false, false, false, false, false, false, false, false, false, false, false, false, false];

% Train a regression model
% This code specifies all the model options and trains the model.
regressionGP = fitrgp (...
 predictors, ...
 response, ...
 'BasisFunction', 'constant', ...
 'KernelFunction', 'squaredexponential', ...
 'Standardize', true);

% Create the result struct with predict function
predictorExtractionFcn = @ (t) t (:, predictorNames);
gpPredictFcn = @ (x) predict (regressionGP, x);
trainedModel.predictFcn = @ (x) gpPredictFcn (predictorExtractionFcn (x));

% Add additional fields to the result struct
trainedModel.RequiredVariables = {'AS', 'AscAo D', 'AscAoD_BSA', 'BAV', 'DLP', 'Female', 'HTN', 'MFS', 'SoV
D', 'Type II Aneurysm', 'WeightLifter', 'age', 'bsa'};
trainedModel.RegressionGP = regressionGP;
trainedModel.About = 'This struct is a trained model exported from Regression Learner R2021b.';
trainedModel.HowToPredict = sprintf ('To make predictions on a new table, T, use: \n yfit = c.predictFcn (T)
\nreplacing "c" with the name of the variable that is this struct, e.g. "trainedModel". \n \nThe table, T, must contain
the variables returned by: \n c.RequiredVariables \nVariable formats (e.g. matrix/vector, datatype) must match the
original training data. \nAdditional variables are ignored. \n \nFor more information, see <a href="matlab:helpview
```

```
(fullfile (docroot, "stats", "stats.map"), "appregression_exportmodeltoworkspace")">How to predict using an
exported model</a>.');

% Extract predictors and response
% This code processes the data into the right shape for training the
% model.
inputTable = trainingData;
predictorNames = {'Female', 'age', 'bsa', 'HTN', 'DLP', 'WeightLifter', 'BAV', 'AscAo D', 'SoV D', 'AscAoD_BSA',
'Type II Aneurysm', 'MFS', 'AS'};
predictors = inputTable (:, predictorNames);
response = inputTable.EnergyLossMeanmeanOfBothAxis;
isCategoricalPredictor = [false, false, false, false, false, false, false, false, false, false, false, false, false];

% Perform cross-validation
partitionedModel = crossval (trainedModel.RegressionGP, 'KFold', 5);

% Compute validation predictions
validationPredictions = kfoldPredict (partitionedModel);

% Compute validation MSE
validationMSE = kfoldLoss (partitionedModel, 'LossFun', 'mse');

end
```

Supplemental Figures

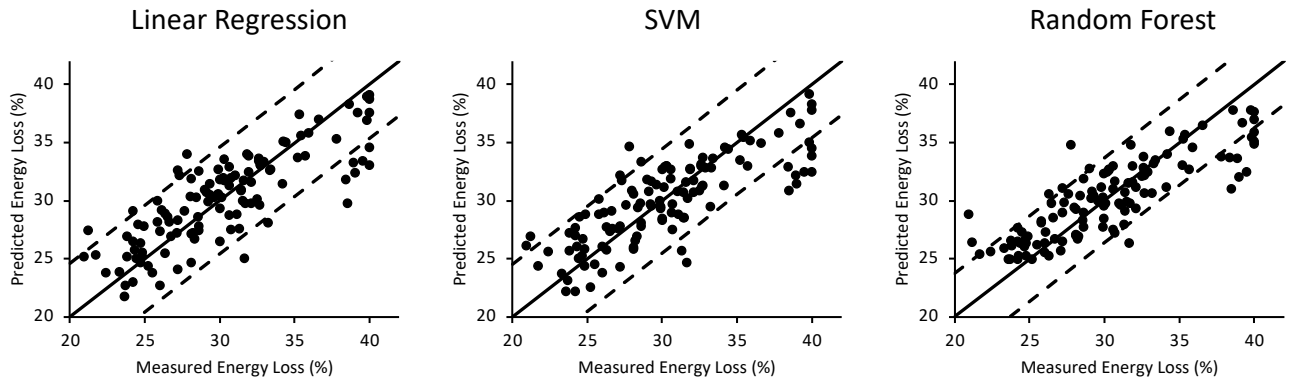

Supplementary Figure 1: Performance plots for non-GPR models.

Model predictions based on clinical predictors. Solid black line indicating line of perfect prediction, dashed lines represent 95% prediction interval. SVM = support vector machine

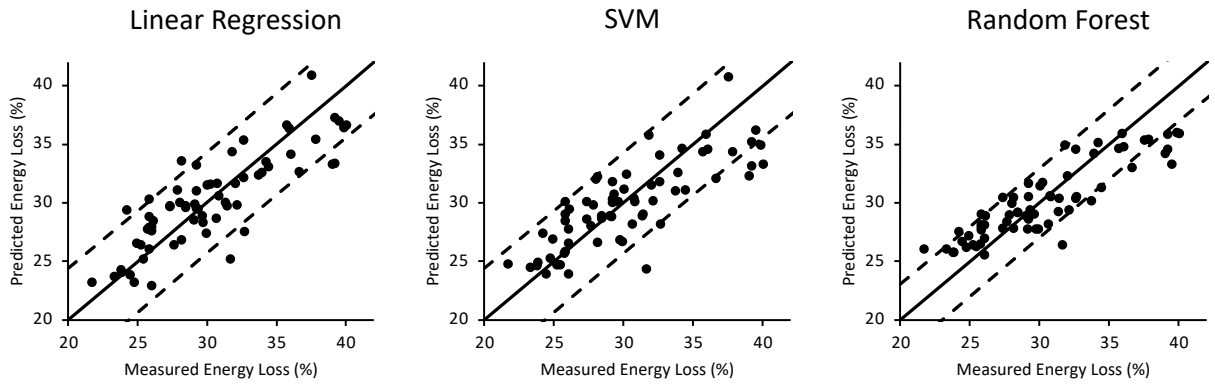

Supplementary Figure 2: Performance plots for non-GPR models considering clinical predictors and CCPM.

Model predictions based on clinical predictors. Solid black line indicating line of perfect prediction, dashed lines represent 95% prediction interval.

SVM = Support vector machine

References

1. Vapnik VN. The Nature of Statistical Learning Theory. New York, NY: Springer New York; 2000.

2. Rasmussen CE, WCKI. Gaussian Processes for Machine Learning. Cambridge, Massachusetts: The MIT Press.; 2006.

3. Breiman L. Random Forests. Machine Learning 2001;45:5–32.

4. Kilic A. Artificial Intelligence and Machine Learning in Cardiovascular Health Care. The Annals of Thoracic Surgery 2020;109:1323–1329.

5. Cuocolo R, Perillo T, de Rosa E, Ugga L, Petretta M. Current applications of big data and machine learning in cardiology. J Geriatr Cardiol 2019;16:601–607.

Chapter 5: Discussion

This thesis aimed to demonstrate the potential for a ML approach to be applied at the clinical level for TAA management, with the motivation of improving the current oversimplified use of size thresholds as the main decisional criteria. The best performing ML algorithm was able to integrate 13 clinically relevant metrics, including different aortic geometries and valve pathologies, comorbidities, and genetic testing results. The correlative performance of the model output to energy loss (R^2:0.63, MSE:8.69) was significantly greater than the correlative performance of aortic size alone (R^2:0.26, MSE:17.5). Moreover, patient age was found to have a stronger relationship to the tissue's energy loss than aortic size-based metrics.

The positive results of this study support the continued pursual of this approach, with the intention of producing a decision support system which is clinically accessible. The limitations of this study demonstrate the heterogeneous nature of the disease and highlight future considerations which should be addressed moving forward.

To advance this approach requires additional data, model development and validation. Firstly, a larger scope study would need to be conducted, whereby patients are recruited from external populations outside of the single research hospital utilized here. In doing so, limitations of the original study with respect to clinical applicability need to be addressed and corrected for moving forward. Following this, a thorough validation process must be conducted to verify the reliability of this method and distinguish if there are limitations to the demographic of patient for whom prediction is reliable. Finally, with the larger scale collection of patients, other types of

input parameters and more complex ML techniques could be considered as an alternative to those utilized here.

Larger Scope Study

The results of the provided study are positive, in that the ML approach provides a correlative measure to mechanical function that is much greater than aortic diameter alone. Many machine learning models are trained using thousands of patients before being considered reliable (94–96). In comparison, a cohort of 158 patients is considered relatively small, however, many regression-based ML algorithms are known to operate well with smaller datasets (106, 107). With this said, the current predictive performance of the models shown are not accurate enough for clinical application. The prediction intervals of widths, 7.4% and 6.4% could presumably be reduced using a larger sized patient cohort. This would also improve the generalizability of the model, as it currently consists of patients from a single center.

The expansion of this study is limited by the use of energy loss as the representative output, in that this eliminates the ability to conduct a large-scale retrospective investigation using publicly available databases. To expand this study, mechanical testing of patients from more diverse demographics needs to be conducted on a larger scale, limiting the pace of progress. The possibility of using other, more widely collected metrics as a representative output, such as observations from histopathological analysis, or a simpler mechanical testing metric, could be considered as an alternative to this approach.

Another alternative approach would be following patients in aortic clinics who do not receive prophylactic surgery, to see if they experience a complication within a given amount of time (ie. 3- or 5- year risk). This could be more easily accomplished as a large-scale study across many different centers, however, the patient population would mainly consist of those who have aortic diameters underneath the surgical threshold and aren't suspected to be at significant risk, as those patients would be operated on. This would help address this group of patients who are experiencing complications below the threshold, which alone is beneficial. However, the question of patients being over the surgical size-threshold while having a stable condition will not be addressed.

In moving forward, consideration to the actual clinical environment in which this technology is intended to be of use needs to be taken into consideration. The study proposed two models, one based solely on clinically accessible data, and the second using a method of speckle tracking TEE. If this device is being considered for application in lower resourced or unspecialized centers, the former model based solely in clinical data would likely be the more applicable option. In this case the model could act as a screening method for referring patients to a specialized clinic. While the model including the speckle tracking analysis will have a higher precision in its predictions, it limits the accessibility of the method. This version of the model would likely be utilized in higher resource and experienced centers, where it will act as an additional tool to supplement decision making.

An additional consideration with respect to required medical imaging, is the need for a consistent measurement technique for aortic geometries. The most common imaging techniques for

evaluating TAA are CTA and MRA(108), however, imaging technique and frequency varies among patients. For those who have had a previous CTA or MRA the amount of time between the imaging date and the date of surgery may allow for residual growth to take place. Every patient who underwent surgical resection underwent a TEE on the day of surgery, which is the reasoning for the use of this method here. However, for this model to be readily applicable in a clinical setting, it is necessary that it is compatible with the imaging techniques which will be most used and considered by clinicians to be most reliable.

Size discrepancy between 2D-TEE measures and CTA have been found to be up to 10%, with TEE being shown to underestimate the aortic size (109). For this reason, it is not practical to simply use these measurement methods interchangeably without correcting for this difference. Additionally, care would need to be given that the measures are consistently being taken at the same point in the cardiac cycle. Measurements within the study were taken at the peak of the QRS interval, however, CTA and MRA images are most commonly taken in diastole (108). The timepoint for measurement largely varies based on the clarity and presence of artifacts in the image. These inconsistencies would need to be addressed to create a model that can be readily integrated into the clinical environment.

Validation Process

The next consideration is the need for a more extensive validation process. Given the highly fatal nature of this disease, the acceptable threshold for trusting a model for this application is very high. Though it is important to note that in the application of this technology, the decision and

care for the patients is still in the hands of the physician, allowing for the ongoing safety monitoring of model predictions.

The use of data from completely external sources will provide validation of the generalizability of the model. Part of model development includes having a firm understanding of which demographics of patients it is applicable to. Studies have shown that models trained on populations having different demographics with respect to race and socioeconomic class have different significant features selected (110). The model produced by this study was created primarily using white patients, and therefore, it's applicability to other demographics is currently unknown. Once a larger and more diverse patient cohort is achieved, care should be taken to determine if there is a difference in the prediction error found amongst patients of different demographics.

Once traditional validation on the model using external data sets has been accomplished, the impact of a model of this nature on clinical practice would need to be assessed in a clinical trial format (85). Comparing the standard of care in ML supported diagnosis to the tradition method. The accuracy of the risk categories approximated by the model compared to those interpreted from aortic diameter can be compared, through histopathological analysis and mechanical testing of the tissue post operatively. The ideal validation process would follow patients to see if they remain stable or undergo a complication, however, this cannot be accomplished without withholding care from at-risk patients. A clinical trial can also assess the confidence and satisfaction of care felt by the clinician and patient when a ML method is being employed (85).

Expanding Modelling Techniques

There are many possibilities for expanding the considered input data to better represent this patient population. Firstly, many previous studies have used supervised learning models with patient blood biomarkers as modelling inputs (23, 24, 99). The addition of this data to the model would be relatively easy to accomplish, as patient blood samples are already collected during surgical intervention. Secondly, one study has demonstrated the ability of a model to consider the rate of change of a patient's condition, through tracking changes in medical records over time (101). This approach could be highly beneficial for the application of TAA, where the growth rate of the aorta is known to be a highly important risk factor (27, 100). Unfortunately, as many patients are incidentally found (10), the number of patients with this data is limited.

One notable limitation within the current study is the handling of BAV patients. For the purposes of the model, this has been treated as a uniform group, however, they are known to be heterogeneous in nature (111). BAV etiology is suspected to have contributions by both genetics and hemodynamics factors (32, 33), having a large range in the progression and anatomical location of aortic dilation, even amongst patients of similar valvular morphology and valve dysfunction levels (112). Phenotypic classifications of BAV patients have been accomplished previously using unsupervised clustering on CTA reconstructions of aortas (90), an approach which could be investigated here as a pretreatment to modelling, to better represent this group.

The collection of a larger number of patients may also allow for the better representation of genetic variants in the patient population. One of the main difficulties with respect to aortopathy is the combination of degenerative and genetic etiologies (113). There are clear hereditable

attributes of the disease, even among individuals who are non-syndromic. Within the scope of the current model, aside from patients having an FBN1 variant, all other variants have a very low incidence with respect the affected gene (breakdown of genetic variants in dataset provided in Appendix A). There are up to 43 known aortopathy genes, each potentially having a unique influence on the biomechanical function of the tissue. Therefore, simply having a single logical input for this group does not appropriately represent their heterogeneity. With a much larger dataset of patients to consider it could be more feasible to consider genetic variants with respect to the type of gene (ie. Affecting extracellular matrix proteins, TGF-beta pathway, etc.), or possibility even with respect to their individual genes.

The heterogeneity within the patient population could possibly be better addressed moving forward using unsupervised clustering (92). Clustering has been shown previously to distinguish between patients having different phenotypes and resultant outcomes for conditions relating to cardiovascular health (88–90). This technique could be utilized as a pre-cursor to supervised learning, in which patients are preemptively separated into groups, for which there are then separate supervised learning models trained. However, the integration of this type of approach would require a much larger patient cohort to be feasible.

With the collection of a larger cohort, this also provides other potential ML algorithms to be explored. This study found the most success using a gaussian process regression algorithm, which are known to be particularly useful on smaller datasets (106). With the collection of larger sums of data, other complex model types, such as neural networks, may be able to provide a better representation of the data (114).

Chapter 6: Conclusions

This thesis details a feasibility study conducted to assess the use of a ML approach for the prediction of TAA tissue biomechanical function. This was accomplished using regression-based ML to predict the energy loss of aortic tissue, as a robust output representing the medial degeneration of the tissue.

This study was guided by the pursuit of the following key research questions:

1. Can ML be used to accurately predict energy loss of TAA patients from only clinical data? How does this prediction compare to other currently used clinical metrics?

Using a cohort of 158 patients, the use of clinical patient data as the only inputs to a machine learning model was shown to give a strong correlative measure to energy loss (R^2: 0.63), which was also justified using an external testing data set. This method demonstrated a significant improvement in correlative performance when compared to the surprisingly poor correlation of size-based metrics alone with energy loss (aortic diameter: $R^2 = 0.26$) and indexed aortic size: $R^2 = 0.32$).

2. What are the key clinical factors that are significant to the model?

Dimensionality reduction techniques used demonstrated that patient age was the most significant factor, greatly surpassing aortic diameter metrics. The valve type of the patient was also shown to be highly significant, which aligns with the current operative guidelines for patients with bicuspid aortic valve (41). These techniques also demonstrated a positive significance in the inclusion of factors relating to patient genetic testing result (such as a diagnosis of Marfan's syndrome), comorbidities (such as hypertension and dyslipidemia),

and patient lifestyle choices (such as heavy weightlifting). Overall, these findings indicated that there is added value in considering a wider scope of patient information beyond aortic diameter when assessing the state of an individual's aortic tissue.

3. Does the inclusion of CCPM improve the prediction of the ML model?

The inclusion of the CCPM as a considered factor was assessed on a cohort of 67 patients. The results demonstrated that the combination of the ML approach using clinical data and CCPM improved the predictive performance of the model further, from R^2:0.46 to R^2:0.62. Combining these two methods gives a greater correlative measure to energy loss than either of the two accomplish individually, with CCPM on its own having R^2:0.53. The inclusion of the CCPM metric mainly improves prediction of patients with very high energy loss values, which was hypothesized to be making up for the lack of information of the tissues' growth rate.

4. What are the main challenges and limitations found by this approach? How feasible would it be for this method to be adopted by the field as a clinical decision support system?

The main limitations of this study are firstly the need for consistency in the data, in a field where there are large variations in treatment and testing between centers. And secondly, the need for a large amount of data to create a reliable model, which is inhibited by the use of energy loss as the ground truth. Strategies have been proposed in the discussion section of this thesis to help address the large heterogeneous nature of the patient population moving forward to better represent these distinct patient groups.

The adoption of this method into the clinical environment for decision marking support would require an extensive validation process, to ensure clinician confidence in the capabilities of the model. As well, the medical imaging derived information being currently considered in the model would need to be refined, to ensure consistency with the measurements that are being routinely taken in the clinic.

Overall, the positive results of this study on this relatively small cohort provides encouragement to the potential of ML in redefining TAA intervention. The value of this approach was clearly demonstrated, supporting the continued expansion of this study moving forward.

References

1. Belz GG. Elastic properties and Windkessel function of the human aorta. Cardiovascular Drugs and Therapy 1995;9:73–83.

2. Ioannou C v., Morel DR, Katsamouris AN, et al. Left Ventricular Hypertrophy Induced by Reduced Aortic Compliance. Journal of Vascular Research 2009;46:417–425.

3. Tintoiu I, Ursulescu A, Elefteriades J, Underwood MJ, Droc I eds. New Approaches to Aortic Diseases from Valve to Abdominal Bifurcation. Elsevier; 2018.

4. Virmani R, Avolio AP, Mergner WJ, et al. Effect of aging on aortic morphology in populations with high and low prevalence of hypertension and atherosclerosis. Comparison between occidental and Chinese communities. Am J Pathol 1991;139:1119–29.

5. Collins JA, Munoz J-V, Patel TR, Loukas M, Tubbs RS. The anatomy of the aging aorta. Clinical Anatomy 2014;27:463–466.

6. Lavall D, Schäfers H-J, Böhm M, Laufs U. Aneurysms of the Ascending Aorta. Deutsches Ärzteblatt international 2012.

7. Chung J, Lachapelle K, Wener E, et al. Energy loss, a novel biomechanical parameter, correlates with aortic aneurysm size and histopathologic findings. The Journal of Thoracic and Cardiovascular Surgery 2014;148:1082–1089.

8. Centers for Disease Control and Prevention. About Multiple Causes of Death, 1999-2019. CDC WONDER Online Database Website 2022.

9. McClure RS, Brogly SB, Lajkosz K, Payne D, Hall SF, Johnson AP. Epidemiology and management of thoracic aortic dissections and thoracic aortic aneurysms in Ontario, Canada: A population-based study. The Journal of Thoracic and Cardiovascular Surgery 2018;155:2254-2264.e4.

10. Booher AM, Eagle KA. Diagnosis and management issues in thoracic aortic aneurysm. American Heart Journal 2011;162:38-46.e1.

11. Wang TKM, Desai MY. Thoracic aortic aneurysm: Optimal surveillance and treatment. Cleveland Clinic Journal of Medicine 2020;87:557–568.

12. Boodhwani M, Andelfinger G, Leipsic J, et al. Canadian Cardiovascular Society Position Statement on the Management of Thoracic Aortic Disease. Canadian Journal of Cardiology 2014;30:577–589.

13. Pape LA, Tsai TT, Isselbacher EM, et al. Aortic Diameter ≥5.5 cm Is Not a Good Predictor of Type A Aortic Dissection. Circulation 2007;116:1120–1127.

14. Clouse WD, Hallett JJW, Schaff H v., Gayari MM, Ilstrup DM, Melton III LJ. Improved Prognosis of Thoracic Aortic Aneurysms. JAMA 1998;280:1926.

15. Coady MA, Rizzo JA, Hammond GL, et al. What is the appropriate size criterion for resection of thoracic aortic aneurysms? The Journal of Thoracic and Cardiovascular Surgery 1997;113:476–491.

16. Emmott A, Garcia J, Chung J, et al. Biomechanics of the Ascending Thoracic Aorta: A Clinical Perspective on Engineering Data. Canadian Journal of Cardiology 2016;32:35–47.

17. Iliopoulos DC, Deveja RP, Kritharis EP, et al. Regional and directional variations in the mechanical properties of ascending thoracic aortic aneurysms. Medical Engineering & Physics 2009;31:1–9.

18. Choudhury N, Bouchot O, Rouleau L, et al. Local mechanical and structural properties of healthy and diseased human ascending aorta tissue. Cardiovascular Pathology 2009;18:83–91.

19. Pierce DM, Maier F, Weisbecker H, et al. Human thoracic and abdominal aortic aneurysmal tissues: Damage experiments, statistical analysis and constitutive modeling. Journal of the Mechanical Behavior of Biomedical Materials 2015;41:92–107.

20. Emmott A, Alzahrani H, Alreshidan M, Therrien J, Leask RL, Lachapelle K. Transesophageal echocardiographic strain imaging predicts aortic biomechanics: Beyond diameter. The Journal of Thoracic and Cardiovascular Surgery 2018;156:503-512.e1.

21. Cuocolo R, Perillo T, de Rosa E, Ugga L, Petretta M. Current applications of big data and machine learning in cardiology. J Geriatr Cardiol 2019;16:601–607.

22. Motwani M, Dey D, Berman DS, et al. Machine learning for prediction of all-cause mortality in patients with suspected coronary artery disease: a 5-year multicentre prospective registry analysis. European Heart Journal 2016:ehw188.

23. Sánchez-Cabo F, Rossello X, Fuster V, et al. Machine Learning Improves Cardiovascular Risk Definition for Young, Asymptomatic Individuals. J Am Coll Cardiol 2020;76:1674–1685.

24. Miranda E, Irwansyah E, Amelga AY, Maribondang MM, Salim M. Detection of Cardiovascular Disease Risk's Level for Adults Using Naive Bayes Classifier. Healthcare Informatics Research 2016;22:196.

25. Marcus GM. The Apple Watch can detect atrial fibrillation: so what now? Nature Reviews Cardiology 2020;17:135–136.

26. Collins MJ, Dev V, Strauss BH, Fedak PWM, Butany J. Variation in the histopathological features of patients with ascending aortic aneurysms: a study of 111 surgically excised cases. Journal of Clinical Pathology 2008;61:519–523.

27. Hiratzka LF, Bakris GL, Beckman JA, et al. 2010 ACCF/AHA/AATS/ACR/ASA/SCA/SCAI/SIR/STS/SVM Guidelines for the Diagnosis and Management of Patients With Thoracic Aortic Disease. Circulation 2010;121.

28. Judge DP, Dietz HC. Marfan's syndrome. The Lancet 2005;366:1965–1976.

29. Loeys BL, Schwarze U, Holm T, et al. Aneurysm Syndromes Caused by Mutations in the TGF-β Receptor. New England Journal of Medicine 2006;355:788–798.

30. Hope MD, Hope TA, Meadows AK, et al. Bicuspid Aortic Valve: Four-dimensional MR Evaluation of Ascending Aortic Systolic Flow Patterns. Radiology 2010;255:53–61.

31. Michelena HI, Khanna AD, Mahoney D, et al. Incidence of Aortic Complications in Patients With Bicuspid Aortic Valves. JAMA 2011;306:1104.

32. Barker AJ, Markl M, Bürk J, et al. Bicuspid Aortic Valve Is Associated With Altered Wall Shear Stress in the Ascending Aorta. Circulation: Cardiovascular Imaging 2012;5:457–466.

33. Debiec R, Sall H, Samani NJ, Bolger A. Genetic Insights Into Bicuspid Aortic Valve Disease. Cardiology in Review 2017;25:158–164.

34. Milewicz DM, Regalado E. Heritable Thoracic Aortic Disease Overview. 1993.

35. Ostberg N, Zafar M, Ziganshin B, Elefteriades J. The Genetics of Thoracic Aortic Aneurysms and Dissection: A Clinical Perspective. Biomolecules 2020;10:182.

36. Davies RR, Gallo A, Coady MA, et al. Novel Measurement of Relative Aortic Size Predicts Rupture of Thoracic Aortic Aneurysms. The Annals of Thoracic Surgery 2006;81:169–177.

37. Zafar MA, Li Y, Rizzo JA, et al. Height alone, rather than body surface area, suffices for risk estimation in ascending aortic aneurysm. The Journal of Thoracic and Cardiovascular Surgery 2018;155:1938–1950.

38. Svensson LG, Khitin L. Aortic cross-sectional area/height ratio timing of aortic surgery in asymptomatic patients with Marfan syndrome. The Journal of Thoracic and Cardiovascular Surgery 2002;123:360–361.

39. Svensson LG, Kim K-H, Lytle BW, Cosgrove DM. Relationship of aortic cross-sectional area to height ratio and the risk of aortic dissection in patients with bicuspid aortic valves. The Journal of Thoracic and Cardiovascular Surgery 2003;126:892–893.

40. Masri A, Kalahasti V, Svensson LG, et al. Aortic Cross-Sectional Area/Height Ratio and Outcomes in Patients With a Trileaflet Aortic Valve and a Dilated Aorta. Circulation 2016;134:1724–1737.

41. Hiratzka LF, Creager MA, Isselbacher EM, et al. Surgery for Aortic Dilatation in Patients With Bicuspid Aortic Valves. J Am Coll Cardiol 2016;67:724–731.

42. Schlatmann TJM, Becker AE. Histologic changes in the normal aging aorta: Implications for dissecting aortic aneurysm. The American Journal of Cardiology 1977;39:13–20.

43. Tsamis A, Krawiec JT, Vorp DA. Elastin and collagen fibre microstructure of the human aorta in ageing and disease: a review. Journal of The Royal Society Interface 2013;10:20121004.

44. Turkbey EB, Jain A, Johnson C, et al. Determinants and normal values of ascending aortic diameter by age, gender, and race/ethnicity in the Multi-Ethnic Study of Atherosclerosis (MESA). Journal of Magnetic Resonance Imaging 2014;39:360–368.

45. Yousef S, Matsumoto N, Dabe I, et al. Quantitative not qualitative histology differentiates aneurysmal from nondilated ascending aortas and reveals a net gain of medial components. Scientific Reports 2021;11:13185.

46. Hosoda Y, Kawano K, Yamasawa F, Ishii T, Shibata T, Inayama S. Age-Dependent Changes of Collagen and Elastin Content in Human Aorta and Pulmonary Artery. Angiology 1984;35:615–621.

47. Gosline J, Lillie M, Carrington E, Guerette P, Ortlepp C, Savage K. Elastic proteins: biological roles and mechanical properties. Philosophical Transactions of the Royal Society of London. Series B: Biological Sciences 2002;357:121–132.

48. Agozzino L, Ferraraccio F, Esposito S, et al. Medial degeneration does not involve uniformly the whole ascending aorta: morphological, biochemical and clinical correlations. European Journal of Cardio-Thoracic Surgery 2002;21:675–682.

49. della Corte A, Quarto C, Bancone C, et al. Spatiotemporal patterns of smooth muscle cell changes in ascending aortic dilatation with bicuspid and tricuspid aortic valve stenosis: Focus on cell–matrix signaling. The Journal of Thoracic and Cardiovascular Surgery 2008;135:8-18.e2.

50. Dietz H, Pyeritz R. Mutations in the human gene for fibrillin-1 (FBN1) in the Marfan syndrome and related disorders. Human Molecular Genetics 1995;4:1799–1809.

51. Halushka MK. Genetic Diseases of the Aorta (Including Aneurysms). In: Cellular and Molecular Pathobiology of Cardiovascular Disease. Elsevier, 2014:239–255.

52. Cotrufo M, della Corte A, de Santo LS, de Feo M, Covino FE, Dialetto G. Asymmetric medial degeneration of the ascending aorta in aortic valve disease: a pilot study of surgical management. J Heart Valve Dis 2003;12:127–33; discussion 134-5.

53. Patel HN, Miyoshi T, Addetia K, et al. Normal Values of Aortic Root Size According to Age, Sex, and Race: Results of the World Alliance of Societies of Echocardiography Study. Journal of the American Society of Echocardiography 2022;35:267–274.

54. Khanafer K, Duprey A, Zainal M, Schlicht M, Williams D, Berguer R. Determination of the elastic modulus of ascending thoracic aortic aneurysm at different ranges of pressure using uniaxial tensile testing. The Journal of Thoracic and Cardiovascular Surgery 2011;142:682–686.
55. Vorp DA, Schiro BJ, Ehrlich MP, Juvonen TS, Ergin MA, Griffith BP. Effect of aneurysm on the tensile strength and biomechanical behavior of the ascending thoracic aorta. The Annals of Thoracic Surgery 2003;75:1210–1214.
56. Iliopoulos DC, Kritharis EP, Giagini AT, Papadodima SA, Sokolis DP. Ascending thoracic aortic aneurysms are associated with compositional remodeling and vessel stiffening but not weakening in age-matched subjects. The Journal of Thoracic and Cardiovascular Surgery 2009;137:101–109.
57. Deplano V, Boufi M, Boiron O, Guivier-Curien C, Alimi Y, Bertrand E. Biaxial tensile tests of the porcine ascending aorta. Journal of Biomechanics 2016;49:2031–2037.
58. Chung J, Lachapelle K, Cartier R, Mongrain R, Leask RL. Loss of mechanical directional dependency of the ascending aorta with severe medial degeneration. Cardiovascular Pathology 2017;26:45–50.
59. Bellini C, Kristofik NJ, Bersi MR, Kyriakides TR, Humphrey JD. A hidden structural vulnerability in the thrombospondin-2 deficient aorta increases the propensity to intramural delamination. Journal of the Mechanical Behavior of Biomedical Materials 2017;71:397–406.
60. Sacks MS. Biaxial Mechanical Evaluation of Planar Biological Materials. Journal of Elasticity 2000;61:199–246.
61. Sokolis DP, Kritharis EP, Giagini AT, Lampropoulos KM, Papadodima SA, Iliopoulos DC. Biomechanical response of ascending thoracic aortic aneurysms: association with structural

remodelling. Computer Methods in Biomechanics and Biomedical Engineering 2012;15:231–248.

62. Cebull HL, Rayz VL, Goergen CJ. Recent Advances in Biomechanical Characterization of Thoracic Aortic Aneurysms. Frontiers in Cardiovascular Medicine 2020;7.

63. Styczynski G, Cienszkowska K, Ludwiczak M, Szmigielski C. Age-related values of aortic pulse wave velocity in healthy subjects measured by Doppler echocardiography. Journal of Human Hypertension 2021;35:1081–1087.

64. Mitchell GF. Imaging Tools in Cardiovascular Research. In: Clinical and Translational Science. Elsevier, 2009:105–121.

65. Baumgartner D, Baumgartner C, Mátyás G, et al. Diagnostic power of aortic elastic properties in young patients with Marfan syndrome. The Journal of Thoracic and Cardiovascular Surgery 2005;129:730–739.

66. Vitarelli A, Giordano M, Germano G, et al. Assessment of ascending aorta wall stiffness in hypertensive patients by tissue Doppler imaging and strain Doppler echocardiography. Heart 2010;96:1469–1474.

67. de Beaufort HWL, Nauta FJH, Conti M, et al. Extensibility and Distensibility of the Thoracic Aorta in Patients with Aneurysm. European Journal of Vascular and Endovascular Surgery 2017;53:199–205.

68. Farzaneh S, Trabelsi O, Chavent B, Avril S. Identifying Local Arterial Stiffness to Assess the Risk of Rupture of Ascending Thoracic Aortic Aneurysms. Annals of Biomedical Engineering 2019;47:1038–1050.

69. Pasta S, Agnese V, di Giuseppe M, et al. In Vivo Strain Analysis of Dilated Ascending Thoracic Aorta by ECG-Gated CT Angiographic Imaging. Annals of Biomedical Engineering 2017;45:2911–2920.

70. Trabelsi O, Gutierrez M, Farzaneh S, Duprey A, Avril S. A non-invasive methodology for ATAA rupture risk estimation. Journal of Biomechanics 2018;66:119–126.

71. Nasr B, le Ven F, Savean J, et al. Characterization of the Physiological Displacement of the Aortic Arch Using Non-Rigid Registration and MR Imaging. European Journal of Vascular and Endovascular Surgery 2017;53:282–289.

72. Rengier F, Weber TF, Henninger V, et al. Heartbeat-related distension and displacement of the thoracic aorta in healthy volunteers. European Journal of Radiology 2012;81:158–164.

73. Soulat G, Scott MB, Allen BD, et al. Association of Regional Wall Shear Stress and Progressive Ascending Aorta Dilation in Bicuspid Aortic Valve. JACC: Cardiovascular Imaging 2022;15:33–42.

74. Krishnan K, Ge L, Haraldsson H, et al. Ascending thoracic aortic aneurysm wall stress analysis using patient-specific finite element modeling of in vivo magnetic resonance imaging. Interact Cardiovasc Thorac Surg 2015;21:471–80.

75. Mahadevia R, Barker AJ, Schnell S, et al. Bicuspid Aortic Cusp Fusion Morphology Alters Aortic Three-Dimensional Outflow Patterns, Wall Shear Stress, and Expression of Aortopathy. Circulation 2014;129:673–682.

76. Hope MD, Hope TA, Crook SES, et al. 4D Flow CMR in Assessment of Valve-Related Ascending Aortic Disease. JACC: Cardiovascular Imaging 2011;4:781–787.

77. Boccadifuoco A, Mariotti A, Capellini K, Celi S, Salvetti MV. Validation of Numerical Simulations of Thoracic Aorta Hemodynamics: Comparison with In Vivo Measurements and Stochastic Sensitivity Analysis. Cardiovascular Engineering and Technology 2018;9:688–706.
78. Capellini K, Vignali E, Costa E, et al. Computational Fluid Dynamic Study for aTAA Hemodynamics: An Integrated Image-Based and Radial Basis Functions Mesh Morphing Approach. Journal of Biomechanical Engineering 2018;140.
79. Phillips EH, di Achille P, Bersi MR, Humphrey JD, Goergen CJ. Multi-Modality Imaging Enables Detailed Hemodynamic Simulations in Dissecting Aneurysms in Mice. IEEE Transactions on Medical Imaging 2017;36:1297–1305.
80. Polanczyk A, Piechota-Polanczyk A, Domenig C, Nanobachvili J, Huk I, Neumayer C. Computational Fluid Dynamic Accuracy in Mimicking Changes in Blood Hemodynamics in Patients with Acute Type IIIb Aortic Dissection Treated with TEVAR. Applied Sciences 2018;8:1309.
81. Mathworks. Introducing Machine Learning. 2016. Available at: https://www.mathworks.com/content/dam/mathworks/tag-team/Objects/i/88174_92991v00_machine_learning_section1_ebook.pdf. Accessed June 16, 2022.
82. Foraker RE, Benziger CP, DeBarmore BM, et al. Achieving Optimal Population Cardiovascular Health Requires an Interdisciplinary Team and a Learning Healthcare System: A Scientific Statement From the American Heart Association. Circulation 2021;143.
83. Friedman CP, Wong AK, Blumenthal D. Achieving a Nationwide Learning Health System. Science Translational Medicine 2010;2.

84. Martin-Isla C, Campello VM, Izquierdo C, et al. Image-Based Cardiac Diagnosis With Machine Learning: A Review. Frontiers in Cardiovascular Medicine 2020;7.

85. Kilic A. Artificial Intelligence and Machine Learning in Cardiovascular Health Care. The Annals of Thoracic Surgery 2020;109:1323–1329.

86. Markets and Markets. Artificial Intellegence in Healthcare Market by Offering, Technology, Application, End User and Geography - Global Forecast to 2027. 2021.

87. Dias RD, Shah JA, Zenati MA. Artificial intelligence in cardiothoracic surgery. Minerva Cardioangiologica 2020;68.

88. Kwak S, Lee Y, Ko T, et al. Unsupervised Cluster Analysis of Patients With Aortic Stenosis Reveals Distinct Population With Different Phenotypes and Outcomes. Circulation: Cardiovascular Imaging 2020;13.

89. Flores AM, Schuler A, Eberhard AV, et al. Unsupervised Learning for Automated Detection of Coronary Artery Disease Subgroups. J Am Heart Assoc 2021;10.

90. Wojnarski CM, Roselli EE, Idrees JJ, et al. Machine-learning phenotypic classification of bicuspid aortopathy. The Journal of Thoracic and Cardiovascular Surgery 2018;155:461-469.e4.

91. Bruse JL, Schievano S, Zuluaga MA, et al. Detecting Clinically Meaningful Shape Clusters in Medical Image Data: Metrics Analysis for Hierarchical Clustering Applied to Healthy and Pathological Aortic Arches. IEEE Transactions on Biomedical Engineering 2017;64:2373–2383.

92. McLachlan G. Cluster analysis and related techniques in medical research. Statistical Methods in Medical Research 1992;1:27–48.

93. Guo T, Fang Z, Yang G, et al. Machine Learning Models for Predicting In-Hospital Mortality in Acute Aortic Dissection Patients. Front Cardiovasc Med 2021;8:727773.

94. Allyn J, Allou N, Augustin P, et al. A Comparison of a Machine Learning Model with EuroSCORE II in Predicting Mortality after Elective Cardiac Surgery: A Decision Curve Analysis. PLOS ONE 2017;12:e0169772.

95. Kilic A, Goyal A, Miller JK, et al. Predictive Utility of a Machine Learning Algorithm in Estimating Mortality Risk in Cardiac Surgery. The Annals of Thoracic Surgery 2020;109:1811–1819.

96. Frizzell JD, Liang L, Schulte PJ, et al. Prediction of 30-Day All-Cause Readmissions in Patients Hospitalized for Heart Failure. JAMA Cardiology 2017;2:204.

97. Daghistani TA, Elshawi R, Sakr S, Ahmed AM, Al-Thwayee A, Al-Mallah MH. Predictors of in-hospital length of stay among cardiac patients: A machine learning approach. International Journal of Cardiology 2019;288:140–147.

98. Ortiz J, Ghefter CGM, Silva CES, Sabbatini RME. One-year mortality prognosis in heart failure: A neural network approach based on echocardiographic data. J Am Coll Cardiol 1995;26:1586–1593.

99. Huo D, Kou B, Zhou Z, Lv M. A machine learning model to classify aortic dissection patients in the early diagnosis phase. Scientific Reports 2019;9:2701.

100. Davies RR, Goldstein LJ, Coady MA, et al. Yearly rupture or dissection rates for thoracic aortic aneurysms: simple prediction based on size. The Annals of Thoracic Surgery 2002;73:17–28.

101. Choi E, Schuetz A, Stewart WF, Sun J. Using recurrent neural network models for early detection of heart failure onset. J Am Med Inform Assoc 2017;24:361–370.

102. Loccoh EC, Joynt Maddox KE, Wang Y, Kazi DS, Yeh RW, Wadhera RK. Rural-Urban Disparities in Outcomes of Myocardial Infarction, Heart Failure, and Stroke in the United States. J Am Coll Cardiol 2022;79:267–279.

103. Zettervall SL, Buck DB, Soden PA, et al. Regional variation exists in patient selection and treatment of abdominal aortic aneurysms. Journal of Vascular Surgery 2016;64:921-927.e1.

104. Schultz WM, Kelli HM, Lisko JC, et al. Socioeconomic Status and Cardiovascular Outcomes. Circulation 2018;137:2166–2178.

105. Onder O, Yarasir Y, Azizova A, Durhan G, Onur MR, Ariyurek OM. Errors, discrepancies and underlying bias in radiology with case examples: a pictorial review. Insights into Imaging 2021;12:51.

106. Rasmussen CE, WCKI. Gaussian Processes for Machine Learning. Cambridge, Massachusetts: The MIT Press.; 2006.

107. James G, Witten D, Hastie T, Tibshirani R. An Introduction to Statistical Learning. New York, NY: Springer New York; 2013.

108. Kallianos KG, Burris NS. Imaging Thoracic Aortic Aneurysm. Radiologic Clinics of North America 2020;58:721–731.

109. Plonek T, Berezowski M, Bochenek M, et al. A comparison of aortic root measurements by echocardiography and computed tomography. The Journal of Thoracic and Cardiovascular Surgery 2019;157:479–486.

110. Segar MW, Jaeger BC, Patel K v., et al. Development and Validation of Machine Learning–Based Race-Specific Models to Predict 10-Year Risk of Heart Failure: A Multicohort Analysis. Circulation 2021;143:2370–2383.

111. Padang R, Bannon PG, Jeremy R, et al. The genetic and molecular basis of bicuspid aortic valve associated thoracic aortopathy: a link to phenotype heterogeneity. Ann Cardiothorac Surg 2013;2:83–91.

112. Nistri S, Sorbo MD, Marin M, Palisi M, Scognamiglio R, Thiene G. Aortic root dilatation in young men with normally functioning bicuspid aortic valves. Heart 1999;82:19–22.

113. Gillis E, van Laer L, Loeys BL. Genetics of Thoracic Aortic Aneurysm. Circulation Research 2013;113:327–340.

114. Alramadhan MM, al Khatib HS, Murphy JR, Tsao K, Chang ML. Using Artificial Neural Networks to Predict Intra-Abdominal Abscess Risk Post-Appendectomy. Annals of Surgery Open 2022;3:e168.

Appendix A: Additional Demographic Information

Table A1: Breakdown of Affected Genes in patient cohort.

Affected Gene	Number of Patients with Positive Variant	Number of Patients with VUS	Total Number of Patients
FBN1	3	2	5
TGFB2	1	1	2
NOTCH1	1	2	3
COL5A2	1	0	1
COL1A1/2	1	1	2
COL5A1	0	1	1
COL3A1	0	2	2
MYH11	0	2	2
ELN	0	3	3
MYLK	0	1	1
FLOD1	0	1	1
CBS	0	1	1
FBLN5	0	1	1
SMAD3	0	1	1
FOXE3	0	1	1
EFEMP2	0	1	1
PLOD1	0	1	1
FL	0	1	1
AA68	0	1	1

*Outside test diagnosed 1 patient with Turner's syndrome, and 1 patient with Noonan syndrome, affected gene unknown.

**Total number of patients with genetic testing is 37 and 3 outside tests, 22 having non-negative results. 1 patient with 2 positive affected genes, 3 patient with 2 VUS genes, 2 patient with 3 VUS genes, 1 patient with 4 VUS genes

Appendix B: Full Performance Results for Dimensionality Reduction Process

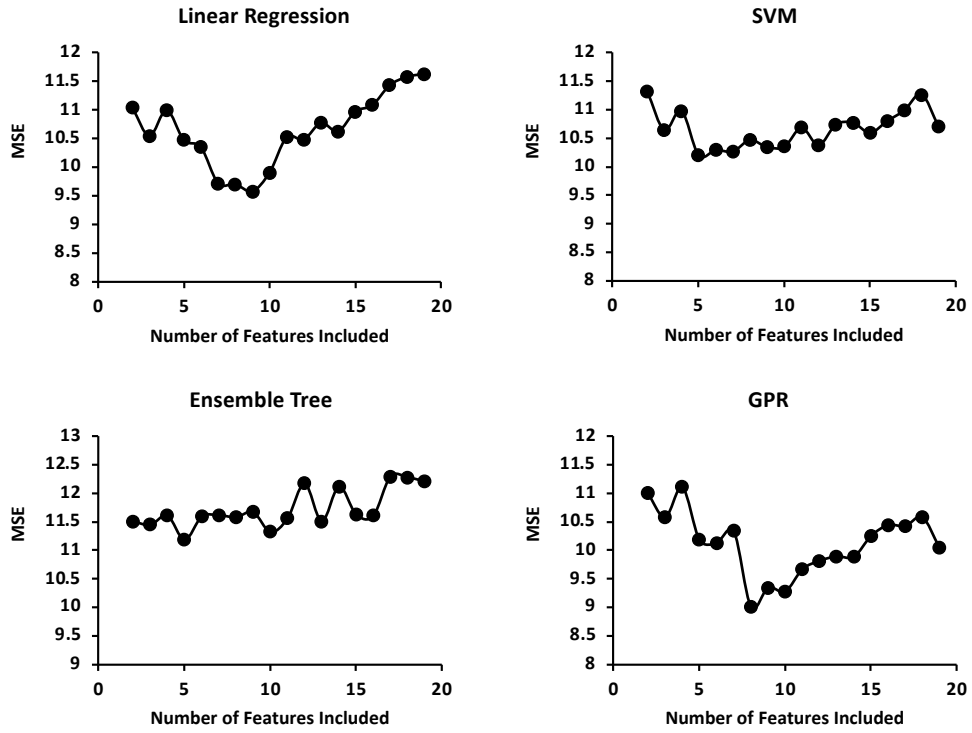

Figure B1: Model performance by MSE as a function of clinical features added in order of f-test ranking.

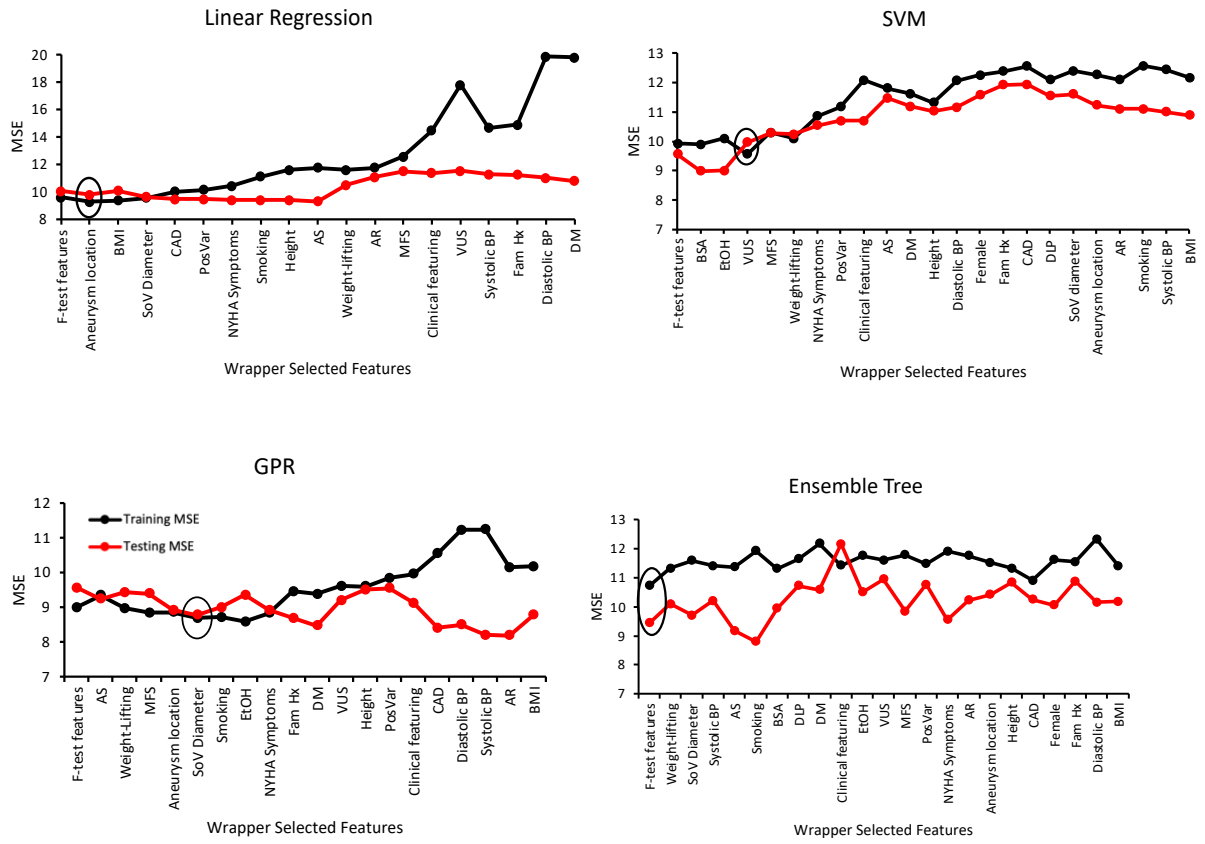

Figure B2: Model performance by MSE as a function of clinical features added by wrapper method. MSE of training data by cross validation shown in black. MSE of testing data shown in red.

Appendix C: Ethics Approval Forms

McGill | Faculty of Medicine and Health Sciences | Faculté de médecine et des sciences de la santé

3655 Sir William Osler #633
Montreal, Quebec H3G 1Y6

3655, Promenade Sir William Osler #633
Montréal (Québec) H3G 1Y6

Tél/Tel: (514) 398-3124

June 14, 2022

Dr. Richard Leask
Department of Chemical Engineering
M. H. Wong Building
3610 University Street
Montreal, QC H3A 2B2

RE: IRB Study Number A06-M62-04B
Aneurysms of the ascending aorta: linking hemodynamics to local tissue stiffness, structure and biochemistry

Dear Dr. Leask,

Thank you for submitting a Continuing Review Form to extend the above-referenced study's ethics oversight for one more year.

The study progress was reviewed and Full Board re-approval was provided on June 13, 2022. The ethics certification renewal is valid to **June 12, 2023**. The status of your renewal submission including documents can be accessed on eRAP. https://infoed.is.mcgill.ca

Investigators are reminded of the requirement to report all McGill IRB approved study documents to the Research Ethics Offices (REOs) of participating study sites, if applicable. Please contact the individual REOs for instructions on how to proceed. Research funds may be withheld and / or the study's data may be revoked for failing to comply with this requirement.

Should any modification or unanticipated development occur prior to the next review, please notify the IRB promptly. Regulation does not permit the implementation of study modifications prior to IRB review and approval.

Regards,

Roberta M. Palmour, PhD
Chair
Institutional Review Board

cc: A06-M62-04B